Cell Therapy & Engineering Connect
ISSN: 3078-3739
2025, Article ID. 2025.0002, Cite as: https://doi.org/10.69709/CellEngC.2024.111335

SCIFINITI

Review Article

OPEN ACCESS

Advances in Microfluidic Bioprinting for Multi-Material Multi-Cellular Tissue Constructs

Rashik Chand[✉,1,2] **Ken-ichiro Kamei**[✉,2,3,4] **Sanjairaj Vijayavenkataraman**[✉,1,2,5,*]

1 The Vijay Lab, Division of Engineering, New York University Abu Dhabi, Abu Dhabi P.O. Box 129188, United Arab Emirates
2 Department of Biomedical Engineering, Tandon School of Engineering, New York University, Brooklyn, NY 11201, USA
3 Programs of Biology and Bioengineering, Divisions of Science and Engineering, New York University Abu Dhabi, Abu Dhabi P.O. Box 129188, United Arab Emirates
4 Institute for Integrated Cell-Material Sciences, Kyoto University, Kyoto 606-8501, Japan
5 Department of Mechanical & Aerospace Engineering, Tandon School of Engineering, New York University, Brooklyn, NY 11201, USA

Article History
Submitted: December 12, 2024 Accepted: January 09, 2025 Published: February 28, 2025

Abstract
3D bioprinting enables fabrication of cell-laden bioinks into complex, biomimetic tissues. However, achieving the spatial and functional heterogeneity of native tissues still poses significant challenges. Microfluidics has emerged as a complementary technology, offering precise control over material flow, mixing, and deposition at the microscale. This review highlights the integration of microfluidics with 3D bioprinting, with a particular focus on the development of advanced "printhead-on-a-chip" systems that enable real-time material switching, gradient formation, and enhanced resolution among other functionalities. Innovations across extrusion, coaxial, droplet-based, light-based, and voxel-based bioprinting modalities are explored, showcasing the transformative potential of microfluidics in creating multifunctional and heterogeneous tissue architectures. Applications in tissue heterogeneity, vascularization, tumor microenvironments, microfiber cellular technology, and organ-on-a-chip systems are discussed, underscoring microfluidics' role in advancing tissue engineering, disease modeling, and drug discovery. Future directions outline the need for scalability, standardization, and simplified workflows that enhance accessibility for broader adoption of microfluidic bioprinting.

Keywords:
bioprinting; microfluidics; 3D printing; tissue engineering

1. Introduction

3D bioprinting is an additive manufacturing technique that constructs cell-laden hydrogels, or bioinks, into functional tissue structures using a layer-by-layer approach (as in extrusion bioprinting) or voxel-by-voxel approach (as in volumetric bioprinting). The primary objective of 3D bioprinting is to create complex, heterogeneous, and biomimetic tissues that closely resemble the architecture and functionality of native biological tissues. Achieving this goal requires the ability to reproduce the spatial and functional heterogeneity found in natural tissues, which often demands the fabrication of multi-material and multi-cellular constructs. This complexity poses unique challenges in material compatibility, cellular integration, and structural stability, particularly when aiming to replicate intricate tissue architectures such as vascular networks or organ-specific microenvironments.

Several bioprinting approaches have been developed to address these challenges, each with distinct advantages and limitations. Common techniques include laser-based bioprinting, droplet-based methods, extrusion-based bioprinting, and stereolithography bioprinting [1]. These methods vary in their precision, scalability, compatibility with bioinks, and suitability for specific applications. However, the discussion of each technique is beyond the scope of this review. The challenges associated with multi-material, multi-cellular tissue fabrication

* **Corresponding Author:**
Sanjairaj Vijayavenkataraman, The Vijay Lab, Division of Engineering, New York University Abu Dhabi, Abu Dhabi, United Arab Emirates, vs89@nyu.edu

is particularly pronounced due to the need to integrate multiple bioinks and cell types within a single construct. Each bioink must exhibit specific properties, such as appropriate viscosity, mechanical properties, and biocompatibility, while ensuring the viability and functionality of embedded cells. Furthermore, ensuring proper spatial arrangement and interaction between different cell types to replicate native tissue complexity remains a significant hurdle. Overcoming these challenges is critical to advancing the field of bioprinting and enabling the fabrication of functional tissues for regenerative medicine, disease modeling, and pharmaceutical testing.

Microfluidics refers to "systems that process or manipulate small (10^{-9} to 10^{-18} L) amounts of fluids, using channels with dimensions of tens to hundreds of micrometers [2]." While initially used for chemical analysis, microfluidics has now been used in a myriad of fields, for example, lab-on-a-chip, organ-on-a-chip, biological assays, sensors, and—the subject of this review—bioprinting, leading to the notion of 'printhead-on-a-chip [3]' or 'lab-on-a-tip [4].' This is partly attributed to its several advantages, such as miniaturization, low volume enabling efficient use of materials, scaling effects like laminar flow due to low Reynolds number, decreased diffusion time, and dominant surface tension and capillary forces [5]. However, fabrication of microfluidic chips remains highly specialized, and the need for bulky supporting components serves as a barrier for widespread adoption. Microfluidics have been used for fabrication of microfibers, however, its incorporation in the additive manufacturing of functional tissue is a relatively recent development. The enhanced control, higher resolution, capability to utilize multiple bioinks, and overall improved macroscopic outcomes make microfluidics a valuable tool for bioprinting.

Conventional methods for tissue engineering rely on a top-down approach, where cells are seeded onto a porous scaffold, prepared from biocompatible and biodegradable materials, with appropriate biologics. Ideally, the seeded cells then migrate and proliferate in the scaffold, eventually replacing the scaffold with their native extracellular matrix [6]. Although this method is relatively straightforward, there are several challenges as well. The scaffold properties depend on the physical and chemical characteristics of the chosen biomaterial. However, cell seeding can be inefficient and time-consuming, often resulting in uneven cellular density within the scaffold. Additionally, replicating the complexity of a three-dimensional tissue environment remains challenging. In contrast to the top-down approach, nature utilizes bottom-up approaches wherein building blocks with nanometer-scale resolution are used to assemble highly complex and functional structures. Replicating this approach in vitro remains a major research interest. Bottom-up approaches in tissue engineering involved creating building blocks using cell encapsulation, cell aggregation, cell sheet, or cell printing. These building blocks can be engineered into larger tissue through various means of assembly [6]. Microfluidic bioprinting could potentially enable bottom-up biofabrication of native tissue microarchitecture and consequently function while overcoming the trade-off between printability and viability [7].

This review will explore the diverse approaches of integrating microfluidics into bioprinting and their transformative impact on the field. The first part will delve into the fabrication of microfluidic nozzles, highlighting key methodologies such as photolithography, 3D printing, and micro-milling, which have enabled the creation of complex and multifunctional designs. It will also examine how microfluidic systems have enhanced or enabled various modalities of 3D bioprinting, namely extrusion-based bioprinting, co-axial bioprinting, droplet-based bioprinting, light-based bioprinting, and voxel-based bioprinting. Special attention will be given to the unique features microfluidics brings to these modalities, including improved resolution, material blending, real-time mixing, controlled material switching, and cell-friendly environments that minimize shear stress. The second part of the review will shift focus to the applications of these microfluidic-enabled modalities. In particular, the use of microfluidic bioprinting for mimicking tissue heterogeneity and vascularization, recapitulating tumor microenvironment, cellular microfibers, and Organ-on-a-Chip will be discussed.

2. Overview of Fabrication of Microfluidic Nozzles

Several methods exist in literature for the fabrication of microfluidic devices, with the choice of technique depending on instrument availability and production requirements [8–10]. Low-volume production may involve casting, laminate manufacturing, laser fabrication, or 3D printing. Techniques such as hot embossing, injection molding, and sheet or film operations are suitable for high production volume. Mechanical methods include Computer Numerical Control (CNC) milling or micro-milling, grinding, and machining (air-jet, water-jet, and ultrasonic), whereas electro-discharge machining, laser ablation, and focused ion beam machining are energy-assisted methods of fabrication. Replication-based methods, such as soft lithography and thermoforming are widely adopted. Depending on the method and material, the achievable roughness, minimum feature size (resolution), and cost are different (Table 1). Three of the commonly used methods for microfluidic nozzle fabrication for bioprinting are discussed below.

2025, Vol. 1, Article ID. 2025.0002
https://doi.org/10.69709/CellEngC.2024.111335

Table 1: Comparison of fabrication method for microfluidic printhead nozzle.

Fabrication Method	Roughness	Minimum Feature Size	Cost
Micro-machining/Micro-milling	High	50 μm	Moderate equipment cost
Photolithography	Low	Sub μm	High for master mold fabrication
3D printing	Moderate	25–50 μm	Low

2.1. Soft Lithography

Soft lithography is a versatile and cost-effective technique used to fabricate microfluidic devices, including microfluidic nozzles, by leveraging elastomeric molds to replicate intricate microscale patterns [11]. An overview of the process is shown in Figure 1A. The process begins with designing the desired pattern, creating a mask, then the master mold, typically using photolithography. This technique, capable of achieving a resolution of approximately 1 μm, defines the desired pattern of the microstructures. Particularly in replica molding (RM), a liquid elastomer, often polydimethylsiloxane (PDMS), is then cast over the master and cured. Once solidified, the PDMS is peeled off, resulting in a flexible mold or replica that mirrors the master's features. PDMS's optical transparency, biocompatibility, and modifiable surface properties make it particularly suitable for applications involving biological and chemical samples [12]. This mold can either be used directly as a microfluidic device or undergo further processing. The advantage of soft lithography is that only the preparation of the master mold requires a clean room, and the same master mold can be used multiple times. Besides RM, there are other patterning techniques, such as microcontact printing (μCP), micro-transfer molding, micromolding in capillary, solvent-assisted micro-molding, and others, which are beyond the scope of this review and have been reviewed elsewhere [8,9].

2.2. Micro-Machining/Micro-Milling

Micro-milling (Figure 1B) is a subtractive manufacturing process that uses rotating cutting tools to create precise microscale features, making it a valuable technique for fabricating microfluidic devices [13]. It supports a variety of materials, including plastics, metals, and glass [14], offering high resolution (down to tens of micrometers) and rapid prototyping by directly machining designs from Computer Aided Design (CAD) models within hours. Advanced setups, such as 5-axis CNC systems [15], enable the creation of complex geometries, such as curved channels, with cost-effective small-batch production compared to injection molding or lithography and <20 μm features. However, limitations include higher surface roughness, tool wear, and difficulty with brittle or elastic materials. Despite these challenges, micro-milling can potentially bridge the gap between low-cost 3D printing and high-precision lithography.

2.3. 3D Printing

The emergence of 3D printing has revolutionized the field of microfluidics by offering a rapid, cost-effective, and versatile alternative to traditional fabrication methods such as soft lithography and PDMS-glass bonding [16]. Conventional manufacturing techniques often require expensive equipment, cleanroom facilities, and extensive expertise, making the process time-intensive and costly. 3D printing addresses many of these challenges by enabling quick prototyping, reduced infrastructure needs, and streamlined workflows. Among the various 3D printing technologies, stereolithography (SLA) stands out for its high precision and ability to produce complex microfluidic devices (Figure 1C). SLA uses a light source to cure photosensitive resin layer by layer, achieving finer resolution (~20 to 250 μm), faster printing time, and higher structural integrity [17]. Multilayer microfluidic devices, which were once laborious to produce, can now be fabricated with reduced footprint and enhanced functionality. Despite its benefits, challenges persist in producing small, multilayered, or highly complex devices. Issues such as unintended curing due to light penetration and the impact of resin properties on the final outcomes require optimization of printer settings or the development of customized resins. With that said, there are commercially available printers, such as the CADworks3D M-series, as well as resins specifically designed for 3D printing microfluidic devices. Additionally, the emergence of open-source design tools specifically for 3D printing of microfluidic devices greatly reduces the complexity of fabrication [18].

3. Incorporation of Microfluidics in Various Bioprinting Modalities

3.1. Extrusion Printing

Extrusion based bioprinting is one of the most widely accessible techniques for biofabrication due to its scalability, printability with viscous bioinks with high cell density, and low cost [19]. However, it faces issues such as

2025, Vol. 1, Article ID. 2025.0002
https://doi.org/10.69709/CellEngC.2024.111335

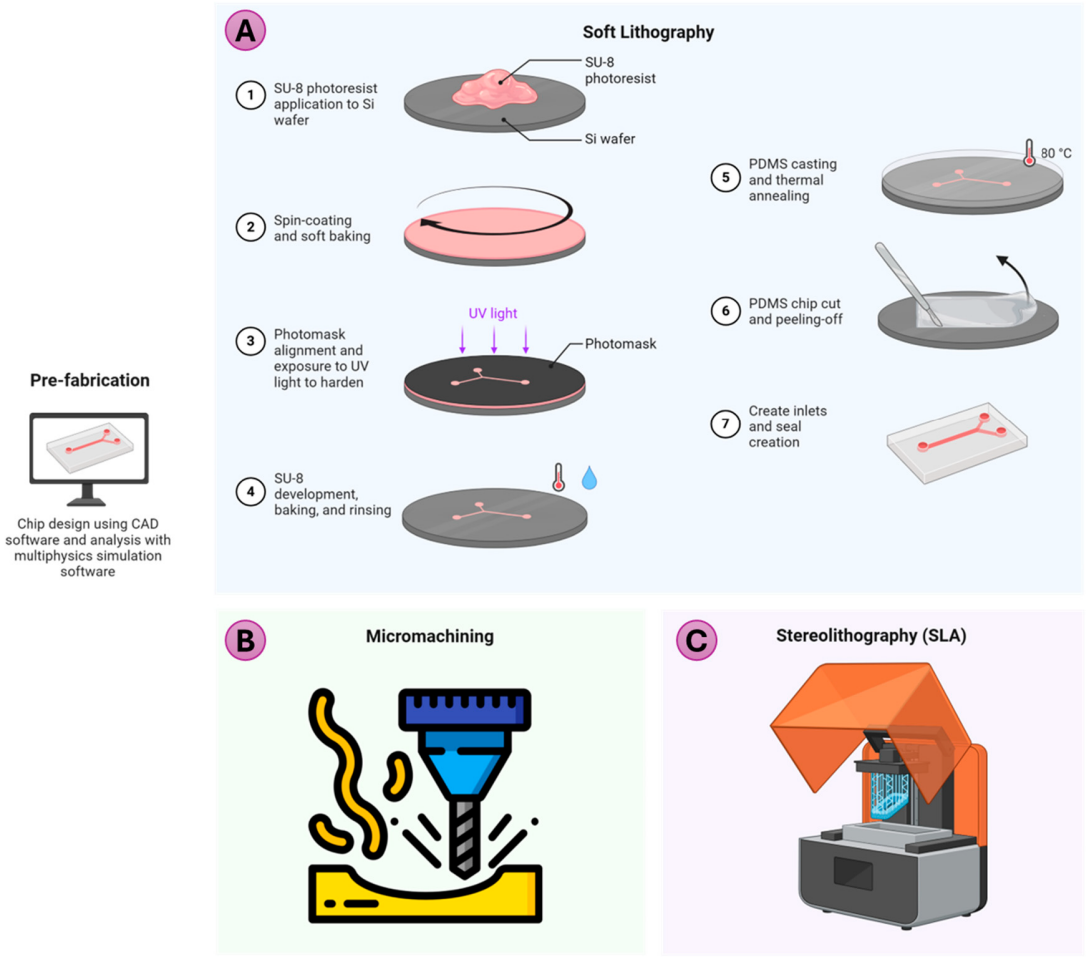

Figure 1: Fabrication methods for microfluidic chips/nozzles. Commonly used methods include (**A**) soft lithography, (**B**) micromachining/micro-milling, and (**C**) stereolithography 3D printing. Prefabrication (3D model preparation) is done using a 3D design software. Image made in BioRender.

lower resolution (few to hundreds of μm), potentially low cellular viability due to wall shear stress during printing, and nozzle clogging [20]. In addition, conventional multi-material extrusion printing requires the use of multiple bioink cartridges and nozzles, making the process tedious. Microfluidic techniques can enhance extrusion bioprinting by improving print resolution, allowing efficient material switching or mixing, and reducing the shear stress exerted on the cells.

A screw-like printhead extruder was used, with viscoelastic materials delivered from two ends via syringe pumps. This setup enabled controlled transitions to create gradients in composition and material properties, as demonstrated by the study conducted by Hardin et al. [21]. Figure 2A,B show possible printed fiber structure using such a method. The printheads were fabricated from acrylic using CNC milling, with two components forming microchannels and two as ink inlets. Solvent welding was used to assemble the polished pieces, with wax (removed later) protecting fine features during the process. The printhead was designed with square channels (hydraulic diameter = 200 μm, length = ~1000 μm), while the microfluidic junction and the final expansion section feature diameters of 200 μm and 400 μm, respectively, with lengths of 200 μm each. The small junction size serves two primary purposes i.e., it enables rapid material switching by minimizing the nozzle's transition volume to around 12.6 nL and mitigates interfacial instabilities, ensuring sharp material transitions. Additionally, a computational model was employed to analyze pressure dynamics, refine the printhead design, and predict flow behavior to achieve precise and seamless transitions between viscoelastic inks in multi-material printing. While the printed PDMS cannot support cells, it does provide a useful proof-of-concept for using other viscoelastic materials.

2025, Vol. 1, Article ID. 2025.0002
https://doi.org/10.69709/CellEngC.2024.111335

Serex et al. used photolithography to fabricate distinct microfluidic nozzle designs to enhance bioprinting capabilities [4]. The material-switching nozzle (Figure 2B) achieved smooth transitions between multiple hydrogels within 500 ms while minimizing dead volume, that is, the volume of fluid remaining in the nozzle after injection. Though valve-based systems could further reduce transition times, they come at the cost of increased ink wastage and extrusion pressure limitations. A microfluidic nozzle incorporating a static herringbone mixer (Figure 2C) was used to mix materials efficiently in laminar flow, enabling gradients in properties such as stiffness or biochemical composition without requiring external energy. A flow-focusing nozzle was used to manipulate fiber width and consequently resolution (Figure 2E). Lastly, a concentrator nozzle (Figure 2F) used crossflow filtering to concentrate microbeads at the outlet by removing excess liquid. Such a design can be used to potentially concentrate cells, minimizing cell loss and shear stress and preserving biological viability. It also allows for the use of low-viscosity solutions, which become concentrated at the nozzle tip. Idaszek and colleagues designed an acrylic-based microfluidic device, manufactured through CNC milling and engraving, incorporating a 40 mm-long serpentine passive mixer integrated with a co-axial extrusion system [22].

Passive mixers can require an extended residence time of fluids to exceed the mixing time constant for effective blending. This issue is particularly pronounced with highly viscous polymers, where the low Reynolds number ($\sim 10^{-5}$) necessitates a mixing channel that can span several meters. Such a large channel results in a substantial priming volume, which is the amount of fluid required to fill the mixing system before it operates effectively. A high priming volume not only delays switching between different material compositions but also leads to material wastage and hinders real-time adjustments. Ober et al. investigated the use of active mixing printheads, incorporating an impeller in the nozzle (Figure 2D), for a range of fluids with different rheology at various flow and mixing rates [23]. By deriving and experimentally verifying novel scaling laws for active mixers, the study demonstrated that mixing strongly viscoelastic fluids in microfluidic channels is achievable at short timescales.

Mani et al. [24] developed a multi-inlet microfluidic nozzle head integrated with shape memory alloy (SMA) actuators for bioprinting. The SMA actuators regulate flow by deforming the PDMS walls of T-shaped microchannels, enabling precise adjustments in flow rates and material composition dynamically. SMA actuators operate at lower voltages, are more cost-efficient than piezoelectric actuators, and eliminate the need for a bulky pneumatic setup.

Microfluidics enables high-throughput printing by using multinozzle arrays to distribute and simultaneously deposit multiple materials (Figure 2G). Hansen et al. used CNC-milling to fabricate an acrylic-based 64-nozzle array, significantly enhancing printing speed and scalability, thereby reducing production times dramatically—for instance, a structure that would take a full day to fabricate with a single nozzle can be completed in just 22 min using a 64-nozzle array [25]. This technology supports the co-printing of materials with diverse rheology, such as viscoelastic wax and Newtonian resins, enabling the creation of complex composite and layered structures. By ensuring uniform deposition, high fidelity, and reproducibility, microfluidics-based high-throughput printing is ideal for applications requiring scalability.

Another application is chaotic bioprinting (Figure 2H), which leverages chaotic advection to create complex, multilayered constructs with high resolution ($\sim$10 μm) and throughput (>1.0 m min^{-1}) [26–29]. Chaotic advection is the creation of small-scale structures in a flow by means of chaotic stretching and folding dynamics, resulting in intricate fractal patterns without requiring high Reynolds numbers, making it ideal for energy-efficient mixing in low-Reynolds-number systems like microfluidics [30,31]. This approach utilizes a Kenics static mixer (KSM), consisting of a series of helicoidal elements within a printhead, to continuously split and fold bioinks, thereby producing well-defined lamellar microstructures. These structures are stabilized via crosslinking, and the number of lamellae, determined as 2 raised to the power of the number of KSM elements, and their thickness can be tuned by varying the KSM elements. The process enhances the surface area of printed structures by increasing perimeter-to-area ratios, which improves diffusive processes and creates localized chemical and physical gradients, and contact-dependent interactions. In chaotic bioprinting, unlike conventional extrusion bioprinting where non-Newtonian bioink rheology minimizes shear stress, bioinks must exhibit Newtonian behavior under specific extrusion conditions to ensure consistent flow dynamics. Hooper et al. [32] introduced CEVIC (Continuously Extruded Variable Internal Channeling) device that makes use of a KSM printhead for high-throughput sheet-based extrusion bioprinting. Besides these, other active and passive (including chaotic) mixer designs have been extensively studied for other microfluidic applications and merit further investigation for use in microfluidic bioprinting [33,34].

Microfluidic mixers have also been employed in the fabrication of cryogels, where the polymer network is formed around frozen solvent ice crystals, which are subsequently removed through thawing [35]. Cryogels are known for their mechanical strength, macroporous structure, and high pore

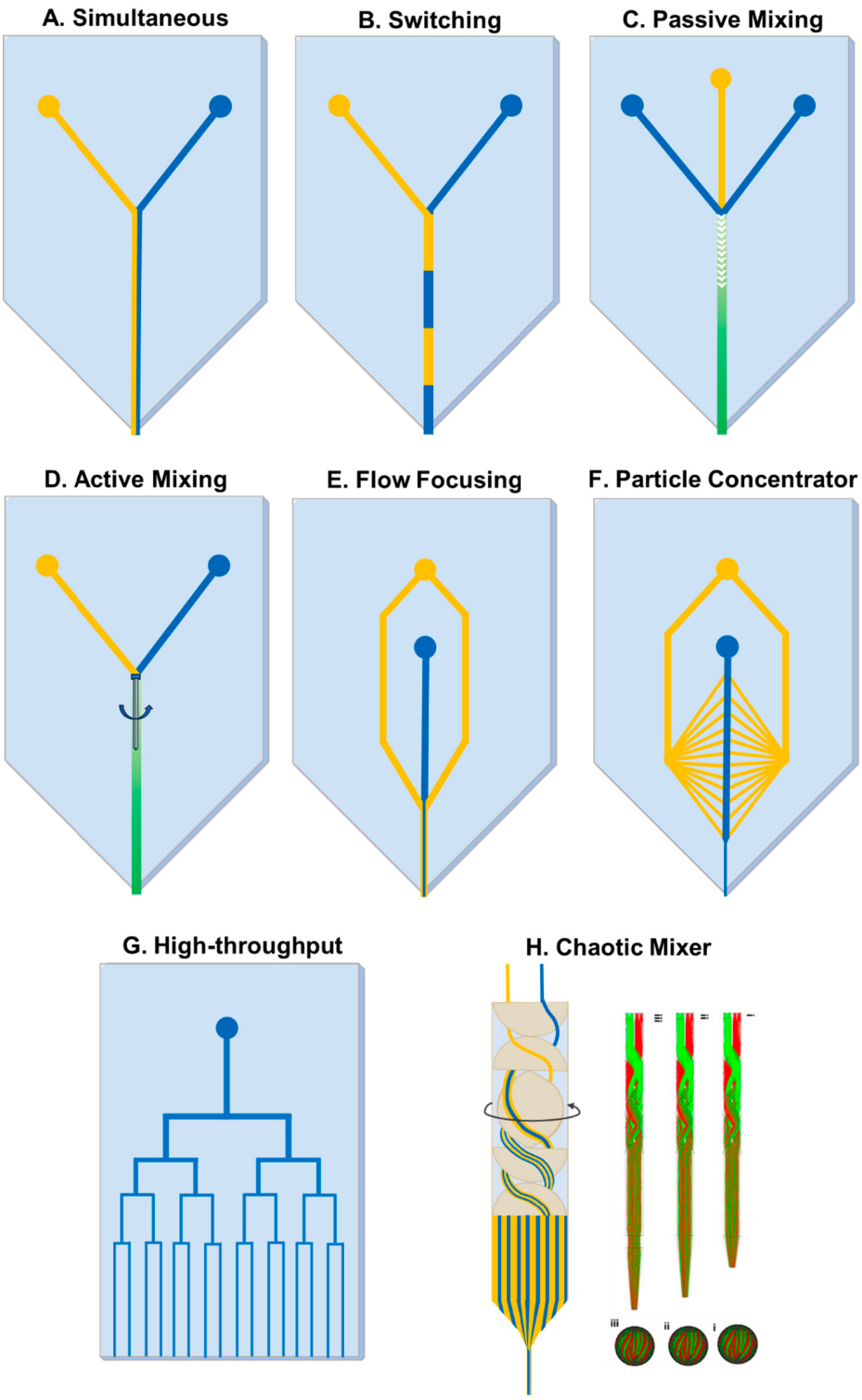

Figure 2: Variation of microfluidic chips/nozzles for extrusion bioprinting. (**A**) Simultaneous extrusion of two bioinks due to laminar flow. (**B**) Switching between two bioinks in a pre-specified manner. (**C**) Passive mixing using a herringbone mixer in the microchannel. (**D**) Use of a propeller for active mixing. (**E**) Flow-focusing microfluidic channel for controlling dispensed filament diameter and reducing shear stress. (**F**) Particle concentrator nozzle for increasing concentration of particles, and possibly cells. (**G**) Multi-array microfluidic nozzle for high throughput printing. (**H**) Chaotic bioprinting using Kenics static mixer (KSM) for chaotic advection. Longitudinal and cross-sectional fiber morphology using different KSM nozzle geometries (**i–iii**). Microstructure (longitudinal and cross section) of the fiber produced using different KSM geometry. Image (**H**) reproduced under CC 4.0 from [26].

2025, Vol. 1, Article ID. 2025.0002
https://doi.org/10.69709/CellEngC.2024.111335

connectivity [36]. The use of microfluidic probes enables precise mixing of cryogenic components just before production, ensuring consistency, and enabling control over pore size by adjusting the temperature in the nozzle.

3.2. Co-Axial Printing

Coaxial printing refers to the use of multi-layered concentric nozzles where each layer can have different materials. The use of microfluidics can mitigate the need for multiple nozzles. Flow-focusing nozzle allowed control over filament diameters, ranging from 800 μm to below 200 μm, by adjusting core and sheath flow rates. This approach eliminated the need for multiple nozzles; however, challenges such as flow instability at high sheath flow rates and excess sheath liquid disrupting printed constructs remain [4]. This also has an additional advantage that cells do not come into direct contact with the nozzle.

Colosi et al. developed a Y-shaped microfluidic chip (Figure 3A) produced using soft lithography and bonding the two PDMS layers containing microchannels (400 μm height, 200 μm width) via plasma bonding [37]. The flow rate of each bioink in the two inlets can be controlled independently using a programmable microfluidic pump. The bioink can be deposited in an alternating sequence or simultaneously, forming a specific parallel pattern, as mixing is prevented because the flow is laminar. It is even possible to switch between alternate and simultaneous deposition in a single construct allowing for a wide range of possible heterogenous structures with unique mechanical properties. The gelatin methacryloyl and alginate bioink was crosslinked using calcium chloride crosslinking solution through a coaxial inlet at the bottom as the bioinks were being extruded and ultraviolet (UV) photocrosslinking after printing.

Beyer et al. [38] fabricated a coaxial 3D printing system for dispensing alginate-based hydrogel with flow focusing and crosslinking with calcium chloride (Figure 3B). The nozzle was fabricated using two complimentary 3D-printed molds onto which PDMS is cast, cured, and bonded. The nozzle also has integrated valves, that are made of a thin PDMS membrane, which allows switching between multiple sources by blocking the channel underneath it upon the application of pneumatic pressure. Cylindrical channel was used as it resulted in more stable fiber and reduced clogging. The alginate bioink is dispensed surrounded by a calcium chloride sheath which crosslinks the alginate and dispenses it as gelled fibers allowing for robust microstructures even while stacking. The resolution of the core alginate bioink can be controlled by varying the sheath flow rate. To prevent the disruption of printing by the accumulation of calcium chloride solution, the structure is printed on a porous surface with a vacuum underneath to remove the extra solution.

Aspect Biosystems has commercialized this microfluidic 3D bioprinting technology through the RX1 bioprinter, featuring the DUO and CENTRA printheads (Figure 3C). The DUO printhead is optimized for dual-material bioprinting, enabling real-time mixing with a crosslinker or buffer solution [39]. In contrast, the CENTRA printhead specializes in fabricating concentric core-shell filaments by co-extruding different bioinks for the core and shell layers, with the outer structure stabilized by a crosslinker [40]. This design allows for the creation of hollow structures by enabling the removal of the core material after fabrication.

Numerous studies have explored microfluidic bioprinting for the fabrication of solid and hollow microfibers suitable for various tissue applications [43–45]. Some methods employ co-axial printing of tubular constructs within a support bath, ensuring structural stability, preventing collapse, enabling the creation of complex geometries, and providing a controlled fabrication environment [46]. As shown in Figure 3D, Pi et al. presented a digitally controlled coaxial extrusion device capable of directly bioprinting complex 3D tubular hollow fibers with multiple circumferential. Using a pressure-assisted system, they were able to continuously fabricate perfusable, tunable structures with monolayer, double-layer, or triple-layer configurations along the tube's length [42]. Remarkably, up to 19 m of acellular mono- and dual-layer hollow conduits have been fabricated in a single bioprinting session without a support bath, utilizing dual crosslinking—a testament to the scalability of this technique [47,48].

3.3. Droplet-Based Printing

Conventional droplet-based 3D bioprinting techniques (inkjet, electro-hydrodynamic jetting, acoustic, microvalve-based bioprinting) face challenges such as limited resolution, inconsistent droplet size, and weak inter-droplet adhesion, which can compromise the structural integrity of printed constructs [1]. Additionally, maintaining cell viability during droplet formation and deposition is difficult.

Microfluidics-enhanced 3D bioprinting can address some of these limitations and has been reviewed in detail by Zhang et al. [3]. Droplet-based microfluidics is a specialized branch of microfluidics that focuses on creating, manipulating, and analyzing tiny liquid droplets within an immiscible carrier fluid [49]. These droplets, typically ranging from femtoliters to nanoliters in volume, act as isolated microreactors, allowing precise control over their size, location, and contents. The technology enables the production of thousands of droplets per second, facilitating high-throughput and parallelized experiments.

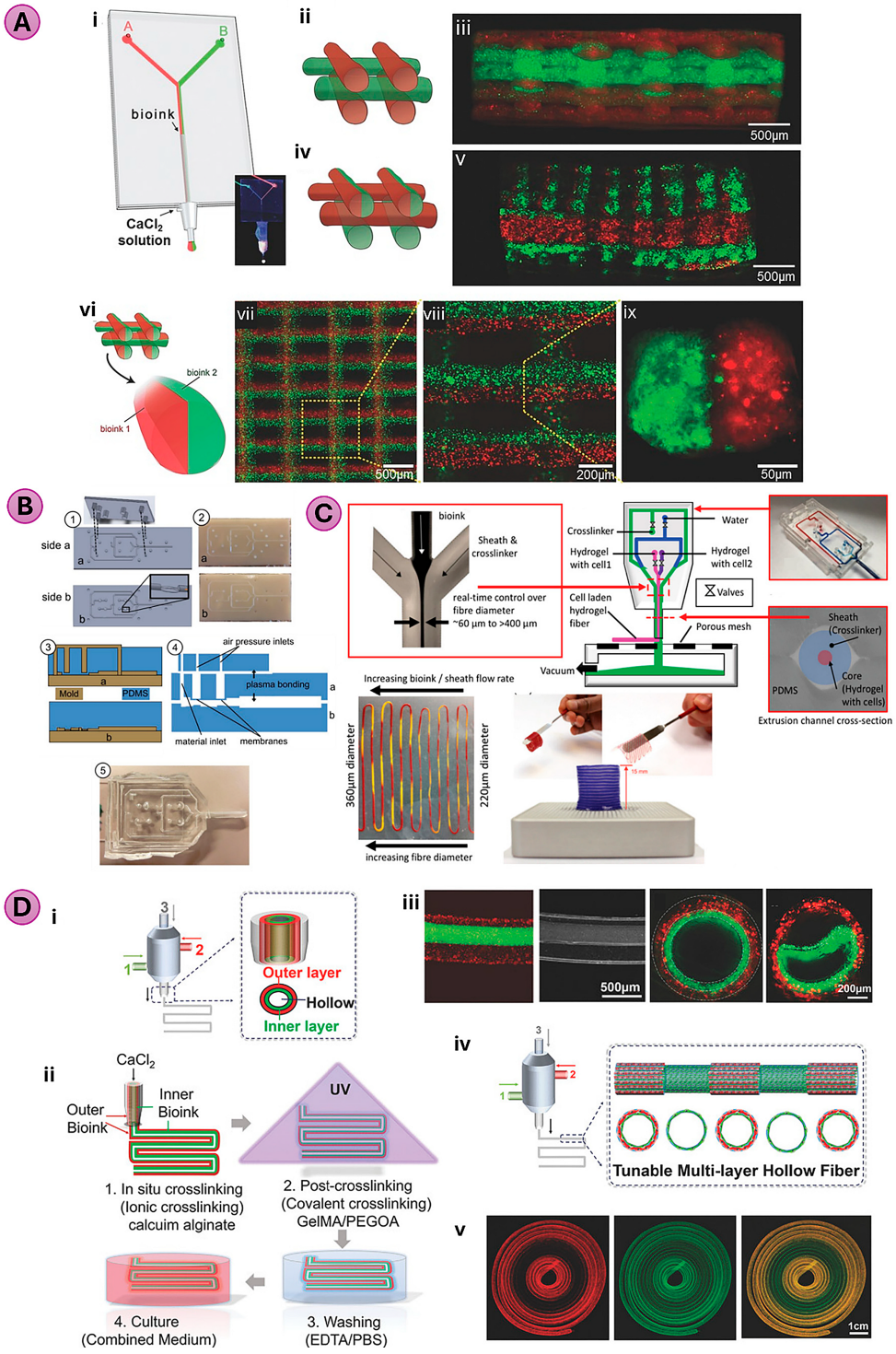

Figure 3: Microfluidics enabled co-axial bioprinting. (**A**) "Y"-shaped channel microfluidic chip connected to a coaxial nozzle (**i**) enabling, alternate deposition (**ii**,**iii**), alternate/simultaneous deposition (**iv**,**v**), and simultaneous (**vi–ix**) hydrogel deposition. Image reproduced with permission from [37]. (**B**) Fabrication of microfluidic printhead using plasma bonded complimentary PDMS halves. The nozzle has a valve membrane and a raised bowl-shaped feature to reduce actuation pressure. Image from [38] (**C**) Schematic of a two-material flow focusing co-axial microfluidic printhead with on-the-fly material switching enabling hydrogel fibers with diameters ranging from approximately 60 to over 400 µm. The porous mesh and vacuum allow for the removal of excessive crosslinker. Image reproduced with permission [41]. (**D**) Schematic of multichannel coaxial extrusion system (**i**) and corresponding bioprinting process with $CaCl_2$ and photocrosslinking (**ii**). Representative longitudinal and cross-sectional image of double-layered perfusable hollow tube with intentional separation also shown (**iii**). Regular switching between single and double layer (**iv**) and florescence imaging of the fabricated construct (**v**). Image reproduced with permission from [42].

2025, Vol. 1, Article ID. 2025.0002
https://doi.org/10.69709/CellEngC.2024.111335

As shown in Figure 4A, Hong et al. combined preset extrusion bioprinting and droplet-based microfluidic emulsification to produce structured, cell-laden microtissue spheroids [50]. In this approach, bioinks are extruded through a compartmentalized coaxial nozzle under controlled conditions, preserving spatial organization and the cross-sectional shape of the structure. The high viscosity of the bioinks and the laminar flow at low Reynolds numbers prevent mixing between compartments, enabling precise patterning. Microfluidics generates uniform droplets by shearing cell-laden bioinks with an immiscible continuous phase, with droplet size controlled through flow rate adjustments. These droplets are thermally gelled without chemical or physical crosslinkers, preserving cellular viability.

Mea et al. employed glass capillary microfluidics to mix immiscible fluid streams (Figure 4B), enabling the printing of 3D print textured constructs with mechanical anisotropy [51]. Similarly, Li et al. utilized a T-junction droplet generator (Figure 4C) to mix two different liquids in a controlled manner, with each liquid independently regulated. The mixture was then dispensed as monodispersed droplets in a continuous immiscible outer liquid, which was incorporated into the final printed structure [52]. This technique enabled the printing of a variety of structures, including 1D composite lines, 2D carpet-like formations, and 3D constructs. Another method involves embedded droplet printing, where two components are mixed, and the resulting droplets are printed within a yield-stress fluid support bath [53]. The bath can either be solidified post-printing or collapsed to retrieve the droplets, depending on the desired application.

Kamperman et al. used "in-air microfluidics" (IAMF), a high-throughput technique to produce monodisperse alginate-based Janus microparticles by colliding liquid microjets in midair (Figure 4D) [54]. Janus particles are uniquely structured microparticles with two distinct compartments, each exhibiting different chemical or physical properties. [55]. IAMF achieves production rates two to three orders of magnitude faster than conventional chip-based methods, enabling precise control over particle size (50–500 μm), compartmentalization, and morphology. The process includes rapid on-the-fly solidification, ensuring structural stability and versatility.

3.4. Light-Based Printing

Traditionally, multi-material printing in SLA and Digital Light Processing (DLP) most commonly relies on sequential resin exchange or replacing the entire resin bath with a new material. In this process, each material is printed layer by layer before draining the resin vat, cleaning the print surface, and refilling the vat with the new material [56]. While this method allows for the fabrication of multi-material structures, it is time-consuming and inefficient, particularly for complex designs. The process often results in material wastage due to residual resin left in the vat or on the print surface, and differences in resin composition can lead to adhesion challenges between layers, potentially compromising structural integrity. Additionally, this approach is limited in its ability to produce smooth material gradients, as it relies on discrete material transitions rather than continuous blending. While light-based bioprinting does not have a nozzle per se, the use of microfluidics for material mixing and switching is desirable.

Miri et al. devised a four-step bioprinting process inside a microfluidic chip for fabricating 3D objects. The process begins with the injection of the selected bioink into the chip's designated printing region, ensuring precise laminar flow and uniform distribution (Figure 5A) [57]. Once the bioink is in position, UV light is applied to photopolymerize and solidify the material layer by layer, forming the desired structure. To maintain clean transitions between different materials, a washing step is performed between layers to remove residual bioink and prevent cross-contamination. Finally, the chip advances vertically to prepare for the next layer, repeating the process with subsequent bioinks or layers until the complete 3D construct is fabricated. A similar approach was taken by Nieto et al. [58] to sequentially dispense two different materials with a washing step in between in a microfluidics working chamber. However, in both approaches, the need for a washing step leads to the wastage of bioink, and the dimensions of the constructs are limited by the microfluidic chip. Extending upon these methods, Wang et al. used a chaotic micromixer that does not just switch but mixes two different biomaterials, allowing for the continuous gradient by tuning the flow rate during the printing process (Figure 5B) [59]. Similarly, Kunwar et al. used a custom-designed microfluidic mixer for supplying the resin during meniscus-enabled projection stereolithography (MAPS) [60].

Han et al. conceived a strategy for multi-material projection micro-stereolithography (PμSL) by replacing the traditional open vat with a pressure-tight fluidic cell. This fluidic cell is controlled by two-way pinch valves to regulate material flow [61]. This innovative material exchange process eliminates the need for a separate washing step by employing pressure-driven flow to replace the previous material, while simultaneously rinsing the printed structure. The process involves injecting the new material into the fluidic cell, flushing out the old material, and repositioning the platform for the next layer, ensuring smooth and clean transitions. Furthermore, this approach enables

2025, Vol. 1, Article ID. 2025.0002
https://doi.org/10.69709/CellEngC.2024.111335

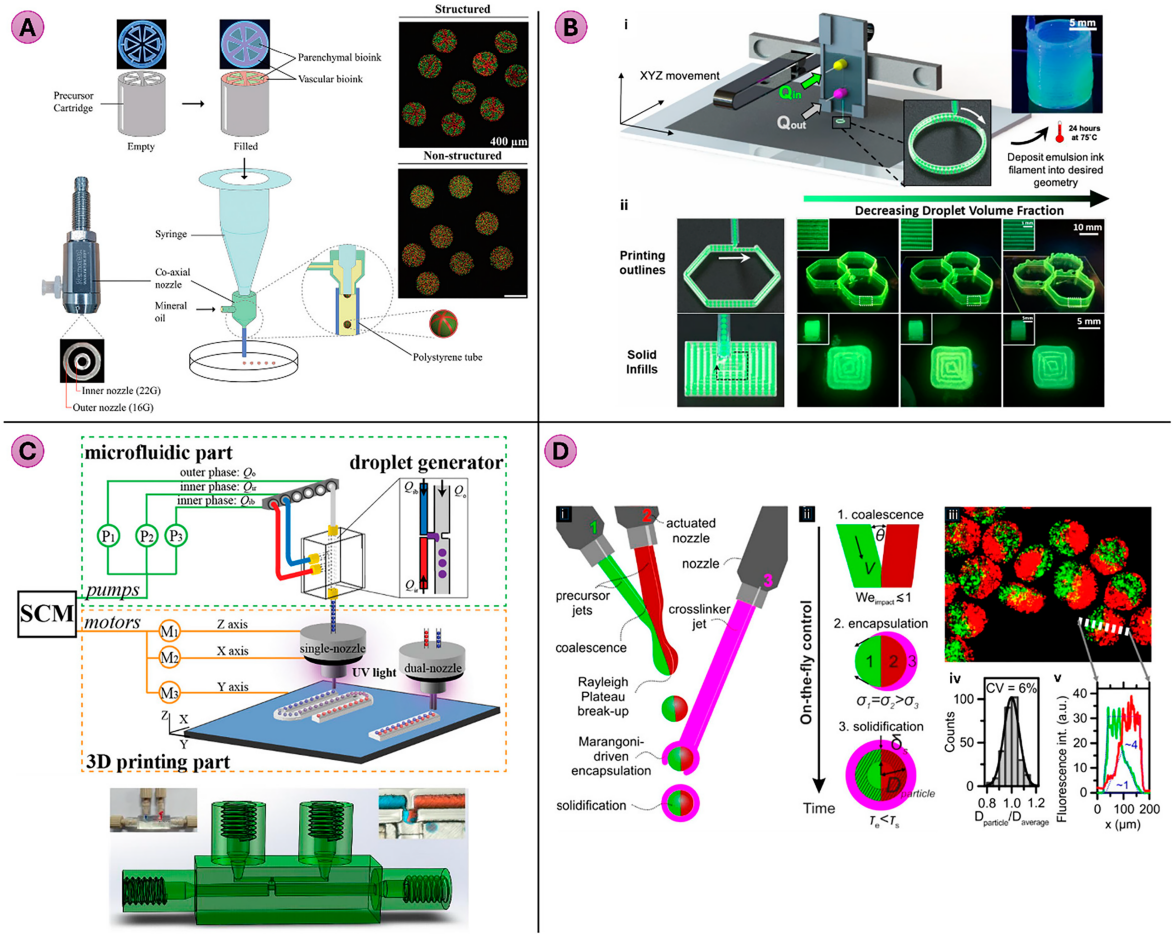

Figure 4: Microfluidics for droplet-based bioprinting. (**A**) Schematic of the combinatorial preset extrusion bioprinting and a microfluidic emulsification system used to fabricate structured and non-structured microtissue spheroids. Reproduced with permission from [50]. (**B**) Process for 3D printing of in situ dispersed aqueous droplets (**i**). (**ii**) Fluorescein imaging shows dispersed droplets in PDMS with droplet volume fraction controlled by changing flow rate. Image reproduced from [51] under PNAS license. (**C**) Schematic of multi-material microfluidic 3D printing platform comprised of a microfluidic module for generating inks with liquid inclusions, a 3D printing module for constructing structures, and a single-chip microcomputer (SCM) for synchronized control. The T-junction droplet generator and the on-demand mixing droplet formation are also shown. Image under CC-BY from [52]. (**D**) Schematic for in-air microfluidics (IAMF) system with two precursor jets (green and red) forming a Janus microjet and a third jet (magenta) providing a cross-linker for encapsulation and solidification (**i**). Janus particles are formed in three major steps: jet and droplet coalescence, surface tension-driven encapsulation, and solidification (**ii**). Microparticles shown in (**iii**) exhibit monodispersed distribution (**iv**) and clear compartmentalization (**v**). Image from [54] under CC-BY-NC-ND.

the integration of multiple materials both layer-by-layer and side-by-side within the same layer, facilitating the fabrication of complex multi-material constructs. More recently, the same group presented a droplet-based resin supply mechanism for PμSL [62].

Fournié et al. developed a novel approach called 3D-FlowPrint, which employs an opto-microfluidic printhead combining hydrodynamic flow confinement (HFC) and photopolymerization using an optical cable [63]. HFC, originally developed for microfluidic probes, is a process where an injected fluid is confined within a controlled flow path by balancing injection and aspiration rates, forming a focused microjet [64]. In bioprinting, this approach effectively recovers excess material from the printing area, reducing contamination in the surrounding medium. Additionally, the photopolymerization process directly projects light onto the material without the need for a vat layer, enhancing precision and material efficiency.

3.5. Voxel-Based Printing

Voxel-based printing transforms 3D fabrication by constructing objects as assemblies of discrete, finite-volume units called voxels, analogous to pixels in 2D images [65]. Each voxel encodes specific material properties, compositions, and structures, enabling highly customizable and

2025, Vol. 1, Article ID. 2025.0002
https://doi.org/10.69709/CellEngC.2024.111335

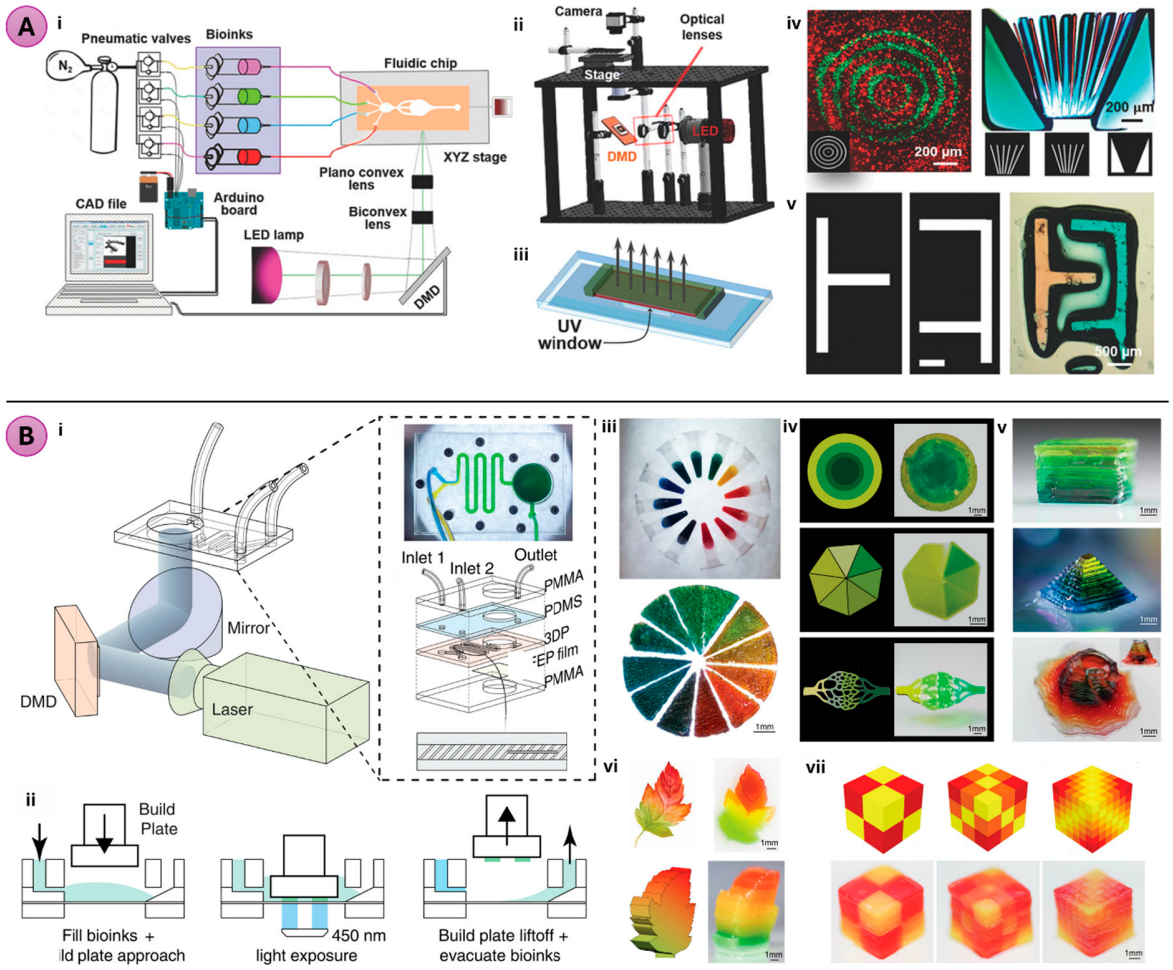

Figure 5: Microfluidics for light-based bioprinting. (**A**) Planar (**i**) and actual (**ii**) schematic for multi-material SLA bioprinting platform comprising of UV lamp (385 nm) for crosslinking, optical lenses and objectives, a digital micromirror device (DMD), and a microfluidic device for material switching. The open-chamber microfluidic chip (**iii**) is used for the printout. (**iv**) Two- and three-component constructs made of GelMA and PEDGA respectively. (**v**) 3D fluidic mixer featuring three distinct colors (white, orange, blue) printed with PEGDA. Reproduced with permission from [57]. (**B**) Composable-gradient DLP bioprinting platform (**i**) integrates a DLP bioprinter with a microfluidic mixing chip that combines multiple bioinks using a chaotic mixing microchannel. (**ii**) Illustration of sequential printing process. Illustrations showing 2D and 3D structures produced via composable-gradient DLP printing, including gradient-colored hydrogels pie (**iii**), 2D patterns with varying gradients (**iv**), and 3D shapes like cubes, pyramids, and vases (**v**). 2D and 3D maple leaf with horizontal and vertical gradient respectively (**vi**). Unit cubes with discrete to continuous gradient (**vii**). Image shown with permission from [59].

intricate designs. By using a virtual n-dimensional matrix as a blueprint, additive manufacturing systems assemble these units to create complex multi-material constructs. Boundary representation and mesh methods are commonly used to represent 3D models for additive manufacturing [66]. However, focusing on external surfaces fails to capture the internal heterogeneity essential for replicating biological tissue architecture. They introduce errors during STL conversion and are computationally inefficient for complex designs with variable properties, often defaulting to homogenized material distributions [67]. In contrast, voxel-based representation encodes detailed internal and external structures, assigning specific properties like material type and porosity to each voxel. In fact, such a voxel-based approach is garnering increased interest through light-based volumetric bioprinting [68]. Even in extrusion printing, a voxel-based approach may simplify fabrication by directly generating 3D printing tool paths, eliminating errors from intermediate steps. Voxel data, derived from medical images such as Computer Tomography (CT) or Magnetic Resonance Imaging (MRI) scans, preserves tissue heterogeneity through processes like image quantization and parametric topology reconstruction, enabling more biomimetic bioprinted constructs [67,69].

While traditional inkjet-based 3D printing has demonstrated voxel-level precision, its limitations in material versatility and resolution have driven the development of alternative methods [65]. Microfluidics have played a pivotal role in advancing voxel-based printing by providing precise control over material flow, mixing, and spatial deposition. Through its ability to handle viscoelastic inks and complex fluid dynamics, microfluidic systems enable the creation of continuous or discrete voxels with tailored compositions in real-time.

Skylar Scott et al. developed a multi-material multi-nozzle (MM3D) printhead with a nozzle diameter of 250 μm, fabricated using a commercially available high-resolution SLA printer (Perfactory Aureus, Envisiontec) with a layer height of 50 μm [70]. The printheads were designed in various configurations, including 4 × 4, 8 × 1, and 16 × 8 nozzle arrays, capable of printing up to eight distinct materials. To address the issue of backflow, where the more viscous silicone ink flowed into the less viscous wax channel, an asymmetric nozzle was introduced with a narrower channel specifically for wax, effectively mitigating the problem. The MM3D printheads demonstrated efficient voxelated printing, with build times that scale linearly with object size (L) rather than cubically (L^3), as seen with single-nozzle systems. The authors reported switching between materials in 16 ms at a print speed of 20 mm/s and a switching frequency of approximately 60 Hz. However, a limitation of the system is that the 3D objects must be produced in periodic layouts, as each nozzle is not independently switchable but instead controlled collectively by a bank of fast-cycling pneumatic solenoids. In addition, the MM3D was capable of printing with gelatin making it a potential option for 3D bioprinting.

In addition to switching between multiple materials, it is often desirable to mix them to create the desired voxel. Hassan et al. demonstrated this by printing UV-curable silicone in a voxelated design using a multi-material microfluidic printhead mixer (MM-PHM) [71]. This printhead, fabricated with a commercial ProJet 2500 Plus 3D printer, comprises an inlet manifold, a mixing chamber, and a metal microneedle with an inner diameter of 230 μm. Two mixing modes were employed: (i) an active pneumatic mixing mode, and (ii) a hybrid mixing routine combining static mixing elements with pneumatic pulses. The MM-PHM was designed with a low length-to-diameter ratio for the nozzle, minimizing dead volume and enabling rapid transitions between material compositions. It was capable of printing a 3D Rubik's cube design consisting of nine different compositions from four different colored materials. While the authors do not investigate biocompatible materials, the UV curing setup could potentially be used for other photocrosslinkable hydrogels.

Voxel-based printing extends beyond extrusion methods to include the voxelated assembly of droplets, a technique known as Digital Assembly of Spherical Particles (DASP) [72]. This method enables the generation, deposition, and assembly of viscoelastic bioinks, overcoming the viscosity limitations of traditional inkjet printing. Unlike droplet generation via Rayleigh-Plateau instabilities, DASP confines and localizes droplets within a sacrificial matrix that can be easily removed after printing, ensuring precise placement and structural integrity. DASP 2.0 has an improved design incorporating dual-network interpenetrating hydrogel droplets, utilizing click chemistry to enhance material versatility and functionality. A significant advantage of DASP is its multiscale porosity: sub-millimeter pores created by the interstitial spaces between particles, and sub-micrometer pores defined by the hydrogel network's mesh size allowing for efficient nutrient diffusion and mechanical robustness.

For DASP 2.0, the printhead includes a dual- or triple-inlet extrusion module (with inner channel dimension narrowing to 425 μm) (Figure 6), fabricated via stereolithography (Formlabs 3+), and includes a static mixer featuring a Quadro™ Square design [73]. The extrusion module is then connected to a standard 26 G nozzle. The dual-inlet nozzle mixes two bioinks in the mixer chamber, while the triple-inlet nozzle introduces a cell suspension to the bioinks before mixing. This versatile system enhances the precision and complexity of printed constructs, enabling the creation of highly organized and functional 3D tissue models.

4. Applications of Microfluidic Bioprinting

Microfluidic bioprinting represents a transformative approach in tissue engineering and regenerative medicine, integrating the principles of microfluidics with advanced bioprinting technologies [48,74,75]. This innovative technique enables the precise manipulation of biological materials at the microscale, facilitating the creation of complex 3D tissue constructs that closely mimic the architecture and functionality of native tissues. As the demand for personalized medicine and organ transplantation continues to rise, effective methods to fabricate viable tissue structures become increasingly critical.

4.1. Tissue Heterogeneity and Vascularization

One of the key advantages of microfluidic bioprinting is its ability to replicate tissue heterogeneity, a critical characteristic of native tissues that is often overlooked in tradi-

2025, Vol. 1, Article ID. 2025.0002
https://doi.org/10.69709/CellEngC.2024.111335

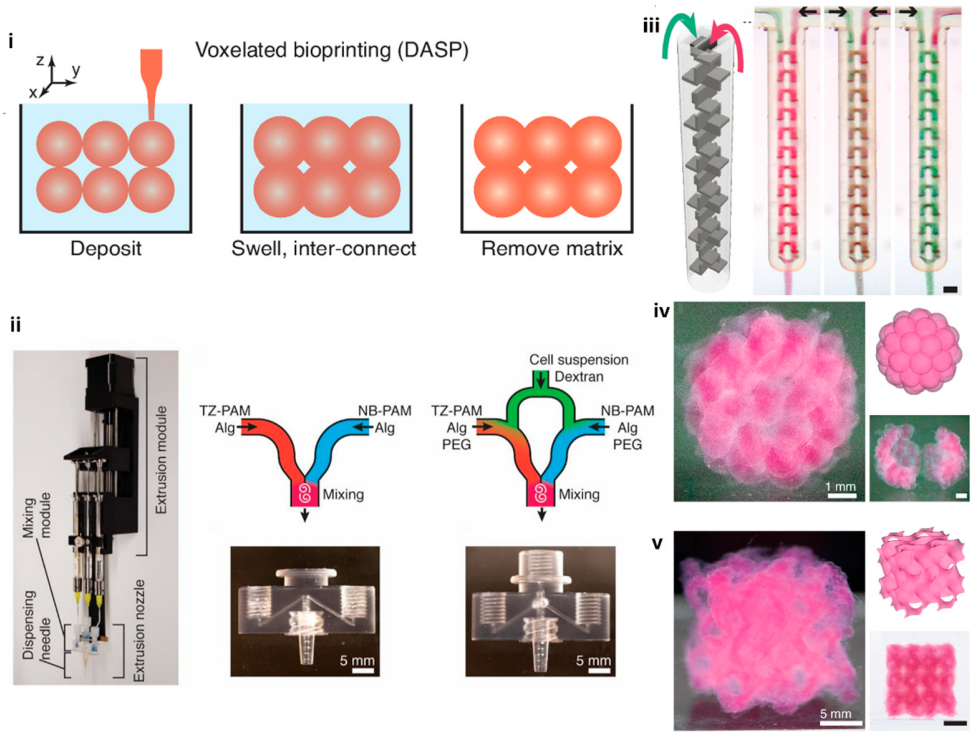

Figure 6: Microfluidics for voxelated bioprinting. (**i**) Digital Assembly of Spherical Particles (DASP) utilizes spherical bioink droplets as building blocks, precisely deposited in a sacrificial yield-stress matrix where they partially coalesce under controlled swelling, then fully crosslink to form free-standing 3D constructs of interconnected yet distinct hydrogel particles. DASP 2.0 enables fabrication with modular double-network (DN) bio-inks. (**ii**) The setup includes an extrusion module with syringes and nozzles, along with dual- and triple-inlet mixing modules. (**iii**) Schematic showing bioinks contain red and green microparticle through passing through the static mixer. (**iv**) A DASP-printed hollow sphere composed of 42 interconnected yet distinguishable hydrogel particles, shown in front view, rendered model, and a cut view. (**v**) A gyroid structure printed with conventional printing using DN hydrogel filaments, depicted from various angles and as a rendered model. Image under CC BY from [73].

tional bioprinting methods. Native tissues are composed of diverse cell types, each with distinct functions, microenvironments, and interactions that contribute to the tissue's overall functionality. Microfluidic bioprinting allows for the precise spatial arrangement of various cell types and biomaterials, enabling the creation of complex tissue constructs that closely mimic the heterogeneous nature of real tissues [74,76,77].

To address these challenges, Costantini et al. tackled the challenge of creating vascular tissues through 3D bioprinting that are mechanically and functionally similar to natural blood vessels [76]. Their method involves a microfluidic printhead coupled with a coaxial needle extruder to create high-resolution hydrogel fibers laden with muscle precursor cells (C2C12). The bioink, composed of polyethylene glycol-fibrinogen (PEG-Fibrinogen), promotes myogenic differentiation, leading to the formation of aligned myotubes that exhibit maturation and functionality. When implanted in vivo, the constructs generated organized muscle-like tissue, demonstrating potential for scaling up skeletal muscle tissue engineering for clinical applications. The introduction of microfluidic control in the bioprinting process allows for precise deposition of bioinks with varied rheological properties—a significant advancement over traditional methods. Despite achieving remarkable muscle structuration at both morphological and functional levels, challenges remain in preserving myo-architecture during in vivo engraftment and scaling the process to human-sized tissues.

Wang et al. also advanced vascular tissue engineering by developing a tough double-network hydrogel bioink for microfluidic bioprinting of mono- and dual-layered hollow conduits, mimicking vein-like and artery-like tissues, respectively (Figure 7) [48]. They introduced a tough double-network hydrogel bioink for microfluidic bioprinting of mono- and dual-layered hollow conduits, mimicking vein-like and artery-like tissues, respectively. The hydrogel, composed of ionically cross-linked alginate and enzyme-cross-linked gelatin, endowed the printed conduits with essential mechanical properties, perfusability, and barrier performance. The arterial conduits demonstrated physiological vasoconstriction and vasodilation

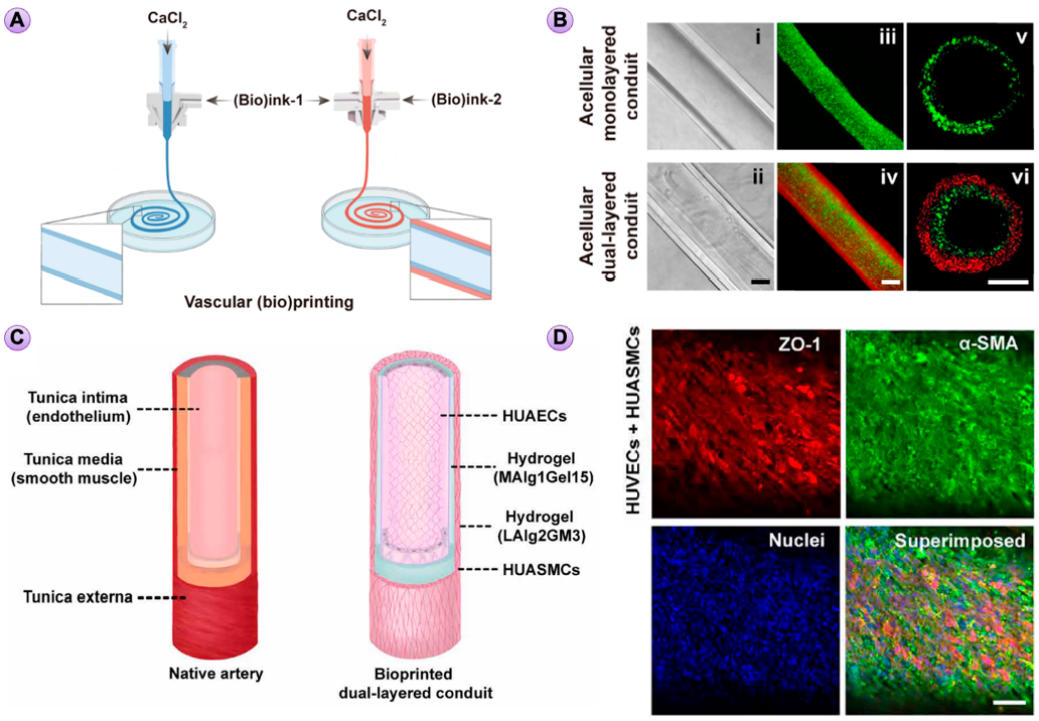

Figure 7: Microfluidic extrusion 3D bioprinting. (**A**) Schematics of microfluidic extrusion (bio)printing of monolayered and dual-layered vascular conduits. (**B**) Representative lateral-view bright-field (**i**,**ii**) and fluorescence microscopic images (**iii**,**iv**), and cross-sectional-view fluorescence microscopic images (**v**,**vi**) of mono-layered (top) and dual-layered (bottom) hollow tubes, respectively. Scale bars, 200 μm. (**C**) Illustration of structures of the native artery and printed arterial conduit. (**D**) Fluorescence confocal images of the immunostained artery exhibiting expressions of ZO-1 by human umbilical artery endothelial cells (HUAECs) and α-SMA by human umbilical artery smooth muscle cells (HUASMCs). The cells were counterstained with DAPI for nuclei. Red, ZO-1; green, α-SMA; blue, nuclei. Scale bars, 100 μm. Reproduced, with permission from [48].

responses, highlighting their potential for vascular anastomosis in disease studies and vascular surgeries. This approach addresses the limitations of previous bioprinted vascular conduits, which were often mechanically weak and unable to withstand physiological pressures. However, the long-term in vivo performance and integration of these bioprinted conduits require further investigation.

Aforementioned, Colosi et al. introduces a Y-shaped microfluidic chip that uses a low-viscosity bioink to create heterogeneous 3D tissue constructs [37]. This method allows for precise deposition and high cell viability, addressing limitations of previous techniques like lack of resolution and limited tissue versatility. The bioink formulation supports cell migration and organization, demonstrated by the successful culture of human umbilical vein endothelial cells (HUVECs) and primary cardiomyocytes, which indicates potential for generating blood vessel-like structures. The technique allows for the creation of multicomponent and multicellular constructs with high definition and cellular behavior, which was not previously established with cell-laden bioinks. The integration of a microfluidic platform enables rapid switching between bioinks, facilitating the creation of complex and heterogeneous tissue fibers on demand.

Collectively, these studies underscore the significant advancements in microfluidic 3D bioprinting, particularly in replicating sophisticated organoids with diverse cell types, including vascular networks. While organoids derived from pluripotent stem cells are also an important method for generating tissue heterogeneity and recapitulating cellular diversity in organs [78–80], they face challenges with reproducibility of organoid structures [81], and the incorporation of vascular networks [82,83]. For instance, brain organoids have shown highly complex structures, but generating proper neural networks across brain organoids with integrated vascular systems still remains challenging [79,84]. Without vascularization, brain organoids often develop necrotic cores due to insufficient nutrient and oxygen diffusion [78,80]. Similarly, kidney organoids are crucial but difficult to recapitulate structurally, given the minute architecture of natural kidneys, which is vital for their function [85,86].

2025, Vol. 1, Article ID. 2025.0002
https://doi.org/10.69709/CellEngC.2024.111335

4.2. Tumor Microenvironments

Microfluidic bioprinting is crucial for replicating tumor microenvironments (TMEs) in vitro. TMEs are complex, comprising cancer cells, immune cells, cancer-associated fibroblasts (CAFs), irregular vasculature, and ECM components [87]. Accurately replicating TMEs is vital for understanding mechanisms of tumor progression, metastasis, and therapeutic resistance [88–97]. However, the heterogeneity and complexity of the TME pose significant challenges to effective cancer treatment and drug development. Traditional 2D models and animal studies often fail to capture these complexities, highlighting the need for advanced modeling techniques.

To tackle this issue, Lee et al. presented a novel approach to constructing a multi-composition tumor array on a single microfluidic device [98] (Figure 8). This device mimics complex transport phenomena within TMEs and allows for the simultaneous evaluation of drug efficacy across 12 distinct conditions. The TME array consists of 36 individual models, each characterized by one of three different compositions and tested under four varying drug concentrations. This study highlights the integration of bioprinting with microfluidics to comprehensively evaluate drug responses across diverse TME conditions. The integration enables the creation of complex TME models on a single platform, facilitating high-throughput drug screening and evaluation of drug efficacy under multiple conditions. The TME models exhibit self-organization into vascular endothelial barriers, which is crucial for studying substance transport and drug penetration in TMEs.

While 3D bioprinting [99] and microfluidic-based cancer-on-a-chip [91,94,100–102] have been reported separately, the combination of microfluidic 3D bioprinting for cancer research remains relatively unexplored Microfluidic 3D bioprinting synergistically merges the advantages of both 3D bioprinting and microfluidic organ-on-a-chip technologies, creating enhanced capabilities for modeling tumor environments. It has been anticipated that more research will emerge in this area, applying these advanced models to better understand TMEs and ultimately leading to advancements in drug discovery.

By integrating the precise spatial control of microfluidics with the structural capabilities of 3D bioprinting, microfluidic 3D bioprinting offers a powerful platform for replicating the complex and heterogeneous nature of TMEs in vitro. This technology addresses the limitations of traditional models that often fail to capture the intricacies of tumor microenvironments. As research in microfluidic 3D bioprinting continues to advance, significant contributions to drug discovery and the development of more effective cancer treatments are expected. This synergy between microfluidics and bioprinting not only enhances the understanding of TMEs but also paves the way for personalized medicine approaches that can improve patient outcomes.

4.3. Microfiber Cellular Technology

Microfiber cellular technology constructs tissue-engineered structures by allowing cells to exhibit intrinsic morphologies and functions similar to living tissues. Microfibers can be assembled into complex 3D structures with organized patterns, essential for mimicking hierarchical tissue organization and reconstructing complex tissues with integrated vascular and neuronal networks.

Onoe et al., fabricated meter-long, cell-laden microfibers using a microfluidic device [103]. Encapsulating extracellular matrix proteins and various cell types, these fibers exhibited tissue functions like muscle contraction and endothelial tubule formation. Assembling these fibers into organized structures offers potential for reconstructing muscle fibers, blood vessels, and nerve networks. In diabetic mice, transplantation of these fibers normalized blood glucose levels, highlighting their therapeutic potential.

Building on this concept, Hassan et al. introduced a microfluidics-based single nozzle printhead equipped with computer-controlled pneumatic pressure valves, allowing for rapid switching between up to seven different bioinks [104] (Figure 9A). This system resolves alignment issues during nozzle switching in traditional bioprinting by using self-healing, biodegradable colloidal gels as support baths (Figure 9B). These gels enhance the spatial organization of bioinks, improve printing fidelity and speed, and provide ECM-like microenvironments for cell growth and host cell invasion (Figure 9C,D). The study successfully printed multicompartment microfibers and complex geometry, demonstrating potential for creating vascularized liver and skeletal muscle tissue constructs. The interconnected microporous networks of colloidal gels maintained complex structures and enabled rapid cell infiltration, supporting tissue integration in vivo.

Pi et al. introduced a significant advancement in bioprinting technology with a multichannel coaxial extrusion system (MCCES) for creating circumferentially multilayered tubular tissues [42]. The MCCES utilizes a digitally coded coaxial extrusion device to directly bioprint three-dimensional complex tubular hollow fibers with multiple circumferential layers. Customized bioinks, including GelMA and alginate, are crosslinked to form stable hollow tubes. This method allows for continuous fabrication of

2025, Vol. 1, Article ID. 2025.0002
https://doi.org/10.69709/CellEngC.2024.111335

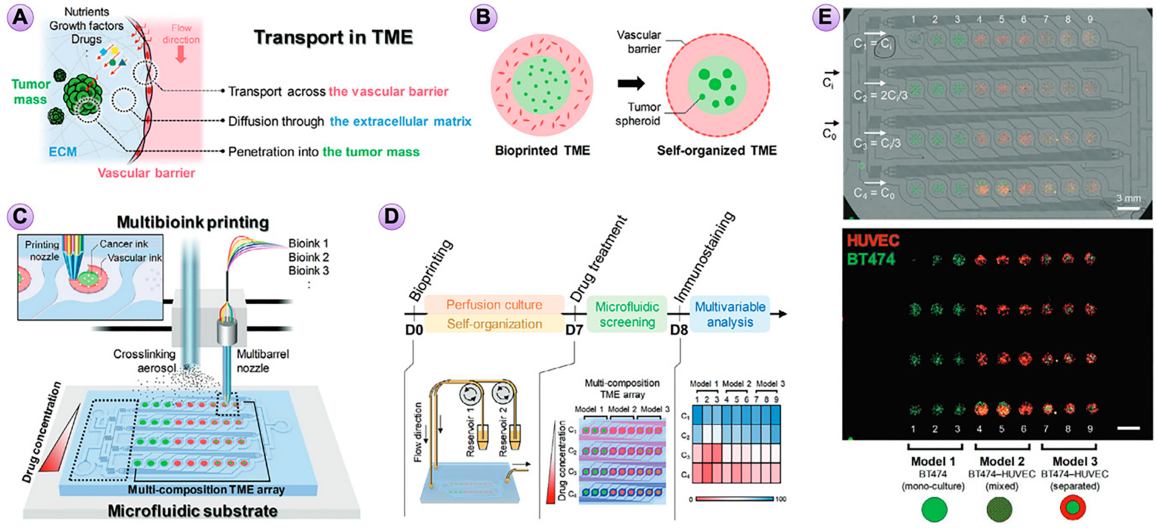

Figure 8: A bioprinted multi-composition TME array on a single microfluidic cell culture for drug screening. (**A**) Illustration of the transport events in the TME. (**B**) Strategic comparison of bioprinted and self-organized TME models composed of a vascular endothelial barrier surrounding tumor spheroids. (**C**) Bioprinting of multi-composition TMEs on a single microfluidic substrate. (**D**) Experimental protocol. (**E**) A multi-composition TME array with the supply medium flow and generates a concentration gradient of the drug. Reproduced, with permission from [98].

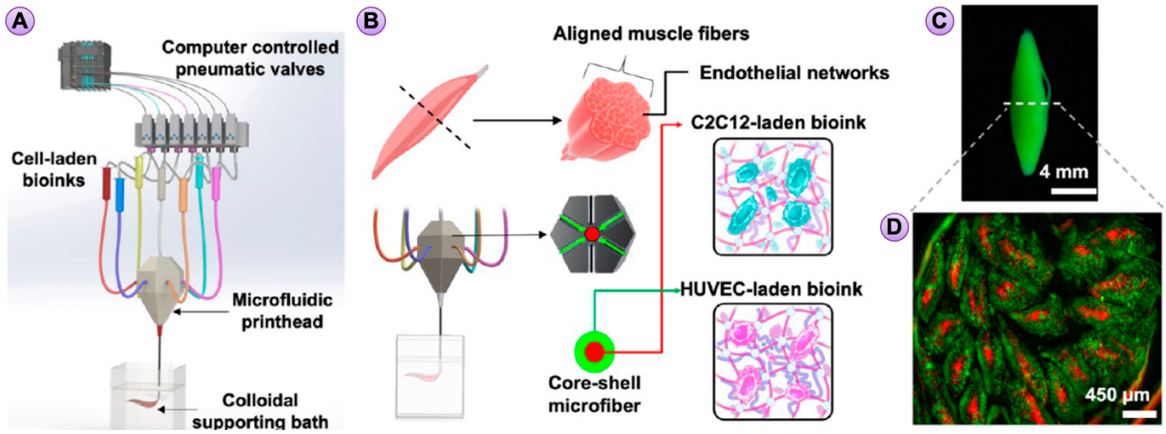

Figure 9: Microfiber cellular technology with microfluidic 3D bioprinting technology. (**A**) Illustration of the bioprinting system showing major components of computer-controlled pneumatic valves, microfluidic single nozzle printhead, and colloidal gel support bath. (**B–D**) Schematics and printed construct of a muscle fiber mimic tissue with a core—shell geometry containing two cell types, C2C12 myocytes and HUVECs, as a shell and core, respectively. Reproduced, with permission from [104].

perfusable and tunable tubular fibers, switching between different layers at regular intervals.

In addressing specific clinical needs, Yin et al. explored the use of 3D bioprinting to create hydrogel structures that mimic the thin epithelial layers of salivary glands (SGs), addressing the unmet need for SG replacement therapy—particularly for xerostomia caused by radiation therapy in head and neck cancer patients [105]. They developed a microfluidics-based coaxial bioprinter capable of fabricating biocompatible hydrogel structures with precise control over dimensions. This flexible platform allows for the printing of both solid fibers and hollow tubes, enabling the incorporation of salivary gland cells at high densities while maintaining cell viability and phenotype. The study demonstrates the potential of these bioprinted structures to replicate the thin epithelia of SGs, marking a significant advancement toward clinical applications. By maintaining high cell viability and precise structural control, this approach opens avenues for restoring SG function through tissue engineering.

Collectively, these studies highlight the potential of microfiber cellular technology in tissue engineering, addressing challenges in creating functional tissues that closely mimic natural counterparts.

2025, Vol. 1, Article ID. 2025.0002
https://doi.org/10.69709/CellEngC.2024.111335

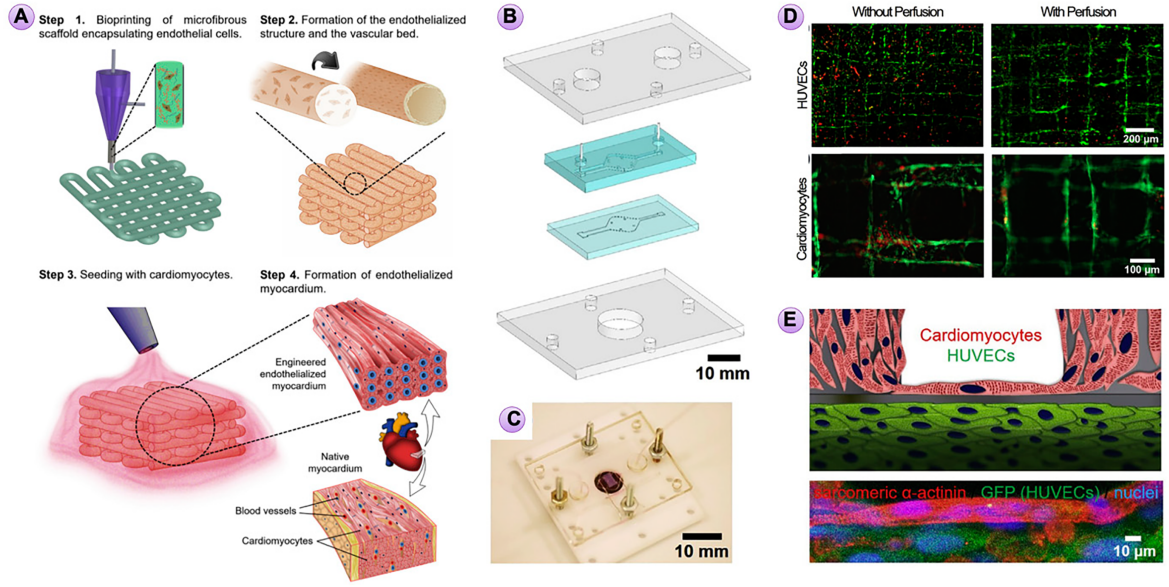

Figure 10: Organs-on-a-Chip platforms established by microfluidic 3D bioprinting technology. (**A**) Schematic illustration of fabricating endothelialized myocardium using the 3D bioprinting strategy. (**B**) Design of the two-layer microfluidic bioreactor sandwiched by a pair of PMMA clamps. (**C**) Photograph of the bioreactor with an embedded bioprinted scaffold. (**D**) Florescent micrographs of LIVE/DEAD staining of bioprinted endothelialized scaffolds without and with perfusion in the microfluidic device. (**E**) Schematic illustration and confocal fluorescence micrograph showing an endothelialized myocardial tissue formed by seeding neonatal rat cardiomyocytes onto the bioprinted endothelialized microfibrous scaffold. Reproduced, with permission from [44].

4.4. Organ-on-a-Chip

Organs-on-a-Chips (OoCs), also known as microphysiological systems (MPSs), simulate physiological functions of human organs, providing accurate environments for studying complex biological processes [106,107]. They offer powerful platforms for drug testing [108,109], disease modeling [110–112], and personalized medicine [112,113].

Integrating microfluidic bioprinting with OoC technology enhances the fabrication of complex tissue structures with precise spatial control. Zhang et al. introduced a bioprinting strategy to construct endothelialized myocardial tissues (Figure 10), crucial for mimicking the natural structure of the myocardium [44]. Their approach allows endothelial cells to migrate and form a confluent endothelium layer within bioprinted microfibers, enhancing the biological relevance of engineered cardiac tissues (Figure 10A). By tuning the macroscale anisotropy of the bioprinted scaffolds, they achieved improved alignment of cardiomyocytes, essential for cardiac tissue engineering. The endothelialized myocardium-on-a-chip model (Figure 10B,C), combined with a microfluidic perfusion bioreactor, offers a promising platform for cardiovascular drug screening, allowing observation of dose-dependent responses in both cardiomyocytes and endothelial cells. The study emphasizes the importance of scaffold design, particularly the aspect ratio of unit grids, in influencing cardiomyocyte maturation, alignment, and contraction—critical for developing functional cardiac organoids (Figure 10D,E).

Pun et al. reported a significant advancement in developing MPSs by introducing GlioFlow3D, a novel platform that combines extrusion bioprinting and stereolithography to mimic the complex tissue environment of glioblastoma (GBM) [114]. This model provides a more accurate system for drug testing by addressing limitations of traditional animal models and PDMS materials that absorb hydrophobic molecules. By integrating primary human cells and GBM cell lines within hydrogel-based microchannels that mimic vasculature and exhibit lower absorption of small molecules, the accuracy of drug testing is improved. Although the study exclusively used fibrin in the hydrogel—which may not fully capture the diverse composition of brain ECMs—future iterations aim to include induced pluripotent stem cell-derived and patient-derived cells. This will improve tumor representation and enhance physiological relevance and clinical translatability. While integrating OoC technology with 3D bioprinting holds great promise for more accurate drug testing and disease modeling by closely mimicking human organ structures, this integration faces significant technical and practical challenges. OoCs require precise microarchitectures to accurately replicate physiological conditions, but current 3D bioprinting technologies struggle to achieve

the necessary microscale features due to limitations in printing resolution. Scaling up production while maintaining consistency and reproducibility is difficult, as variations in printing processes can lead to inconsistencies in tissue structure and function. The complexity of combining both technologies increases manufacturing time and costs, limiting widespread adoption at this stage.

Additionally, the lack of standardized protocols for integrating 3D bioprinting with OoC technologies hampers comparison across studies and model validation. Technical hurdles include replicating precise microarchitectures and dynamic environments, material limitations of bioinks, difficulties in integrating complex microfluidic channels and sensors, and the need for high-resolution printing capabilities. Ensuring cell viability and function, achieving scalability and reproducibility, and navigating regulatory hurdles all add further complexity. Overcoming these challenges requires advancements in bioprinting technology, materials science, a deeper understanding of tissue biology, and effective interdisciplinary collaboration.

5. Conclusions and Future Directions

Microfluidics has undoubtedly garnered interest for enhancing existing 3D bioprinting techniques and enabling new ones. Its most extensive application has been in extrusion bioprinting, enabling diverse configurations for bioink switching [4,21], mixing [22,23,26], and high throughput dispensing [25]. In coaxial printing, microfluidics has facilitated the high-throughput fabrication of multi-layered hollow and solid constructs [37,42]. However, the fabrication of branched structures continues to pose significant challenges. Droplet-based microfluidic printing represents a major advancement over conventional inkjet bioprinting by supporting a broader range of materials, including bioinks with higher viscosities [50–52,54]. Additionally, microfluidics has driven innovation in light-based bioprinting, enabling not only material switching between discrete layers but also the creation of continuous gradient structures [59] and, more recently, intra-layer material switching [63]. Lastly, microfluidics-enabled voxel-based printing holds promise for producing more biomimetic structures that replicate the heterogeneity of natural tissues.

The use of microfluidics for handheld and in situ bioprinting is another exciting advancement. These approaches aim to print functional tissues directly at the site of need, such as during surgical procedures or wound repair, offering significant potential for personalized and adaptable tissue engineering [115,116]. Handheld systems could enable portable solutions for printing complex tissue constructs with high precision in dynamic environments. However, challenges such as scaling down microfluidic systems to portable formats, maintaining stable bioink delivery, and ensuring consistency under variable conditions must be addressed to fully realize their potential.

While these advancements highlight the transformative potential of microfluidics in bioprinting, significant limitations still persist. The widespread adoption of extrusion-based bioprinting is largely attributed to its simplicity and user-friendly nature. In contrast, microfluidic bioprinting remains a specialized technique, hindered by high initial costs due to the need for advanced equipment and expertise. This cost barrier limits accessibility and hinders broader implementation. Additionally, the lack of standardized protocols for integrating microfluidics with 3D bioprinting complicates reproducibility and cross-study comparisons. However, recent developments have improved the accessibility of microfluidic technologies. Open-source tools now facilitate the design of microfluidic channels [18], 3D printing has streamlined the fabrication of microfluidic devices for prototyping [16], and designs for entire microfluidic bioprinters are now available [117]. These advancements are gradually reducing the technical and financial barriers associated with microfluidic bioprinting, paving the way for its wider adoption and integration into 3D bioprinting.

To enhance the effectiveness of microfluidic bioprinting, leveraging computational simulations with experimental verification, to optimize process parameters and analyze the fluid dynamic behavior of microfluidic nozzle designs presents significant potential [63,118,119]. Such simulations, done in silico using software such as COMSOL and ANSYS Fluent, are routinely used to study flow behavior in other microfluidic applications. These methods provide crucial insights into key printing parameters, including nozzle diameter, bioink rheology, nozzle geometry, flow behavior, and shear stress effects on cells. Relationship between the different parameters can then be identified and validated with empirical data. This method offers a promising pathway for improving nozzle designs, addressing challenges like flow instability, and enhancing cellular viability by identifying optimal print parameters in a more systematic manner compared to just trial-and-error.

An underexplored avenue in bioprinting research is the implementation of modular microfluidics, which utilizes standardized components from a library of modules that can be interconnected and customized for specific applications [120,121]. The development of modular microfluidics platforms for bioprinting could lead to standardized, plug-and-play methods that streamline complex

workflows. Similarly, the incorporation of active components into microfluidic nozzles offers significant potential for precise fine-tuning and enhanced control [23,24], but it does so at the cost of simplicity.

Scaling microfluidic bioprinting for larger constructs, while maintaining the exceptional control over the microarchitecture of fabricated constructs enabled by microfluidics-enhanced bioprinting, is another pressing challenge [122]. The integration of microfluidic techniques to embed functional vasculature is particularly critical, as vascularization is essential for nutrient delivery, waste removal, and tissue viability. This includes developing scalable methods that preserve architectural precision while ensuring the functionality of embedded vascular networks. Achieving this goal will be pivotal for more function in vitro tissue models and translating bioprinted tissues into clinical applications.

In summary, microfluidics has led to several exciting developments in 3D bioprinting technologies enabling precision, versatility, and innovation in fabricating multi-material, multi-cellular constructs. However, there are still limitations, such as scalability, cost, and standardization, that need to be addressed. Future advancements will require interdisciplinary efforts to address existing limitations, including vascularization, and explore new frontiers such as modular designs for ease of adaptation. By tackling these challenges, microfluidics-enhanced bioprinting can evolve from a specialized tool into a robust, scalable platform, unlocking new possibilities in bioprinting of complex, heterogeneous tissues with integrated vascular networks, moving closer to the clinical realization of fully functional engineered tissues.

Abbreviations

CNC	Computer Numerical Control
RM	Replica Molding
PDMS	Polydimethylsiloxane
μCP	MicroContact Printing
CAD	Computer Aided Design
SLA	Stereolithography
SMA	Shape Memory Alloy
KSM	Kenics Static Mixer
CEVIC	Continuously Extruded Variable Internal Channeling
UV	Ultraviolet
IAMF	In-Air Microfluidics
DLP	Digital Light Processing
MAPS	Meniscus-Enabled Projection Stereolithography
PμSL	Projection Micro-Stereolithography
HFC	Hydrodynamic Flow Confinement
CT	Computer Tomography
MRI	Magnetic Resonance Imaging
MM3D	Multi-Material Multi-Nozzle
MM-PHM	Multi-Material Microfluidic Printhead Mixer
DASP	Digital Assembly of Spherical Particles
PEG	Polyethylene Glycol
HUVEC	Human Umbilical Vein Endothelial Cell
TME	Tumor Microenvironments
MCCES	Multichannel Coaxial Extrusion System
SG	Salivary Glands
OOC	Organs-On-A-Chip
MPS	Microphysiological Systems
GBM	Glioblastoma

Author Contributions

Conceptualization: R.C. and S.V.; writing—original draft preparation: R.C. and K.-i.K.; writing—review and editing: R.C., K.-i.K. and S.V. All authors have read and agreed to the published version of the manuscript.

Consent for Publication

The authors affirm that no human research participants were involved in this review paper.

Conflicts of Interest

The authors declare no conflicts of interest regarding this manuscript.

Funding

This work was supported by the New York University Abu Dhabi (NYUAD), Faculty Research Fund (AD366 to KK).

Acknowledgments

The author acknowledges New York University Abu Dhabi (NYUAD) for its support and research funding.

References

[1] Vijayavenkataraman, S.; Yan, W.-C.; Lu, W.F.; Wang, C.-H.; Fuh, J.Y.H. 3D bioprinting of tissues and organs for regenerative medicine. *Adv. Drug Deliv. Rev.* **2018**, *132*, 296–332. [CrossRef]

[2] Whitesides, G.M. The origins and the future of microfluidics. *Nature* **2006**, *442*, 368–373. [CrossRef] [PubMed]

[3] Zhang, P.; Liu, C.; Modavi, C.; Abate, A.; Chen, H. Printhead on a chip: Empowering droplet-based bioprinting with microfluidics. *Trends Biotechnol.* **2024**, *42*, 353–368. [CrossRef] [PubMed]

[4] Serex, L.; Bertsch, A.; Renaud, P. Microfluidics: A new layer of control for extrusion-based 3D printing. *Micromachines* **2018**, *9*, 86. [CrossRef]

[5] Sackmann, E.K.; Fulton, A.L.; Beebe, D.J. The present and future role of microfluidics in biomedical research. *Nature* **2014**, *507*, 181–189. [CrossRef] [PubMed]

[6] Lu, T.; Li, Y.; Chen, T. Techniques for fabrication and construction of three-dimensional scaffolds for tissue engineering. *Int. J. Nanomed.* **2013**, *8*, 337–350. [CrossRef] [PubMed]

[7] Nie, M.; Takeuchi, S. Bottom-up biofabrication using microfluidic techniques. *Biofabrication* **2018**, *10*, 044103. [CrossRef]

[8] Scott, S.; Ali, Z. Fabrication methods for microfluidic devices: An overview. *Micromachines* **2021**, *12*, 319. [CrossRef] [PubMed]

[9] Niculescu, A.-G.; Chircov, C.; Bîrcă, A.C.; Grumezescu, A.M. Fabrication and applications of microfluidic devices: A review. *Int. J. Mol. Sci.* **2021**, *22*, 2011. [CrossRef] [PubMed]

[10] Liu, X.; Sun, A.; Brodský, J.; Gablech, I.; Lednický, T.; Vopařilová, P.; Zítka, O.; Zeng, W.; Neužil, P. Microfluidics chips fabrication techniques comparison. *Sci. Rep.* **2024**, *14*, 28793. [CrossRef]

[11] Qin, D.; Xia, Y.; Whitesides, G.M. Soft lithography for micro- and nanoscale patterning. *Nat. Protoc.* **2010**, *5*, 491–502. [CrossRef] [PubMed]

[12] McDonald, J.C.; Whitesides, G.M. Poly(dimethylsiloxane) as a material for fabricating microfluidic devices. *Acc. Chem. Res.* **2002**, *35*, 491–499. [CrossRef] [PubMed]

[13] Guckenberger, D.J.; De Groot, T.E.; Wan, A.M.D.; Beebe, D.J.; Young, E.W.K. Micromilling: A method for ultra-rapid prototyping of plastic microfluidic devices. *Lab A Chip* **2015**, *15*, 2364–2378. [CrossRef]

[14] Hwang, J.; Cho, Y.H.; Park, M.S.; Kim, B.H. Microchannel fabrication on glass materials for microfluidic devices. *Int. J. Precis. Eng. Manuf.* **2019**, *20*, 479–495. [CrossRef]

[15] Modarelli, M.; Kot-Thompson, D.; Hoshino, K. 5-axis CNC micro-milling machine for three-dimensional microfluidics. *Lab A Chip* **2025**, *25*, 127–142. [CrossRef]

[16] Nielsen, A.V.; Beauchamp, M.J.; Nordin, G.P.; Woolley, A.T. 3D printed microfluidics. *Annu. Rev. Anal. Chem.* **2020**, *13*, 45–65. [CrossRef] [PubMed]

[17] Dhand, A.P.; Davidson, M.D.; Burdick, J.A. Lithography-based 3D printing of hydrogels. *Nat. Rev. Bioeng.* **2024**. [CrossRef]

[18] Zhang, Y.; Li, M.; Tseng, T.-M.; Schlichtmann, U. Open-source interactive design platform for 3D-printed microfluidic devices. *Commun. Eng.* **2024**, *3*, 71. [CrossRef]

[19] Zhang, Y.S.; Haghiashtiani, G.; Hübscher, T.; Kelly, D.J.; Lee, J.M.; Lutolf, M.; McAlpine, M.C.; Yeong, W.Y.; Zenobi-Wong, M.; Malda, J. 3D extrusion bioprinting. *Nat. Rev. Methods Primers* **2021**, *1*, 75. [CrossRef]

[20] Chand, R.; Muhire, B.S.; Vijayavenkataraman, S. Computational fluid dynamics assessment of the effect of bioprinting parameters in extrusion bioprinting. *Int. J. Bioprint.* **2022**, *8*, 545. [CrossRef]

[21] Hardin, J.O.; Ober, T.J.; Valentine, A.D.; Lewis, J.A. Microfluidic printheads for multimaterial 3D printing of viscoelastic inks. *Adv. Mater.* **2015**, *27*, 3279–3284. [CrossRef] [PubMed]

[22] Idaszek, J.; Costantini, M.; Karlsen, T.A.; Jaroszewicz, J.; Colosi, C.; Testa, S.; Fornetti, E.; Bernardini, S.; Seta, M.; Kasarełło, K.; et al. 3D bioprinting of hydrogel constructs with cell and material gradients for the regeneration of full-thickness chondral defect using a microfluidic printing head. *Biofabrication* **2019**, *11*, 044101. [CrossRef]

[23] Ober, T.J.; Foresti, D.; Lewis, J.A. Active mixing of complex fluids at the microscale. *Proc. Natl. Acad. Sci. USA* **2015**, *112*, 12293–12298. [CrossRef] [PubMed]

[24] Mani, K.; Lin, W.-C.; Wang, C.-F.; Panigrahi, B.; Wu, Y.-J.; Wu, C.-L.; Chen, C.-Y. A multi-inlet microfluidic nozzle head with shape memory alloy-based switching for biomaterial printing with precise flow control. *BioChip J.* **2020**, *14*, 340–348. [CrossRef]

[25] Hansen, C.J.; Saksena, R.; Kolesky, D.B.; Vericella, J.J.; Kranz, S.J.; Muldowney, G.P.; Christensen, K.T.; Lewis, J.A. High-throughput printing via microvascular multinozzle arrays. *Adv. Mater.* **2013**, *25*, 96–102. [CrossRef]

[26] Chávez-Madero, C.; De León-Derby, M.D.; Samandari, M.; Ceballos-González, C.F.; Bolívar-Monsalve, E.J.; Mendoza-Buenrostro, C.; Holmberg, S.; Garza-Flores, N.A.; Almajhadi, M.A.; González-Gamboa, I.; et al. Using chaotic advection for facile high-throughput fabrication of ordered multilayer micro- and nanostructures: Continuous chaotic printing. *Biofabrication* **2020**, *12*, 035023. [CrossRef]

[27] Ceballos-González, C.F.; Bolívar-Monsalve, E.J.; Quevedo-Moreno, D.A.; Lam-Aguilar, L.L.; Borrayo-Montaño, K.I.; Yee-de León, J.F.; Zhang, Y.S.; Alvarez, M.M.; Trujillo-de Santiago, G. High-throughput and continuous chaotic bioprinting of spatially controlled bacterial microcosms. *ACS Biomater. Sci. Eng.* **2021**, *7*, 2408–2419. [CrossRef] [PubMed]

[28] Bolívar-Monsalve, E.J.; Ceballos-González, C.F.; Borrayo-Montaño, K.I.; Quevedo-Moreno, D.A.; Yee-de León, J.F.; Khademhosseini, A.; Weiss, P.S.; Alvarez, M.M.; Trujillo-de Santiago, G. Continuous chaotic bioprinting of skeletal muscle-like constructs. *Bioprinting* **2021**, *21*, e00125. [CrossRef]

[29] Ceballos-González, C.F.; Bolívar-Monsalve, E.J.; Quevedo-Moreno, D.A.; Chávez-Madero, C.; Velásquez-Marín, S.; Lam-Aguilar, L.L.; Solís-Pérez, Ó.E.; Cantoral-Sánchez, A.; Neher, M.; Yzar-García, E.; et al. Plug-and-play multimaterial chaotic printing/bioprinting to produce radial and axial micropatterns in hydrogel filaments. *Adv. Mater. Technol.* **2023**, *8*, 2202208. [CrossRef]

[30] Aref, H.; Blake, J.R.; Budišić, M.; Cardoso, S.S.S.; Cartwright, J.H.E.; Clercx, H.J.H.; El Omari, K.;

Feudel, U.; Golestanian, R.; Gouillart, E.; et al. Frontiers of chaotic advection. *Rev. Mod. Phys.* **2017**, *89*, 025007. [CrossRef]

[31] Stroock, A.D.; Dertinger, S.K.W.; Ajdari, A.; Mezić, I.; Stone, H.A.; Whitesides, G.M. Chaotic mixer for microchannels. *Science* **2002**, *295*, 647–651. [CrossRef] [PubMed]

[32] Hooper, R.; Cummings, C.; Beck, A.; Vazquez-Armendariz, J.; Rodriguez, C.; Dean, D. Sheet-based extrusion bioprinting: A new multi-material paradigm providing mid-extrusion micropatterning control for microvascular applications. *Biofabrication* **2024**, *16*, 025032. [CrossRef] [PubMed]

[33] Bayareh, M.; Ashani, M.N.; Usefian, A. Active and passive micromixers: A comprehensive review. *Chem. Eng. Process.—Process Intensif.* **2020**, *147*, 107771. [CrossRef]

[34] Cai, S.; Jin, Y.; Lin, Y.; He, Y.; Zhang, P.; Ge, Z.; Yang, W. Micromixing within microfluidic devices: Fundamentals, design, and fabrication. *Biomicrofluidics* **2023**, *17*, 061503. [CrossRef] [PubMed]

[35] Serex, L.; Braschler, T.; Filippova, A.; Rochat, A.; Béduer, A.; Bertsch, A.; Renaud, P. Pore size manipulation in 3D printed cryogels enables selective cell seeding. *Adv. Mater. Technol.* **2018**, *3*, 1700340. [CrossRef]

[36] Jones, L.O.; Williams, L.; Boam, T.; Kalmet, M.; Oguike, C.; Hatton, F.L. Cryogels: Recent applications in 3D-bioprinting, injectable cryogels, drug delivery, and wound healing. *Beilstein J. Org. Chem.* **2021**, *17*, 2553–2569. [CrossRef]

[37] Colosi, C.; Shin, S.R.; Manoharan, V.; Massa, S.; Costantini, M.; Barbetta, A.; Dokmeci, M.R.; Dentini, M.; Khademhosseini, A. Microfluidic bioprinting of heterogeneous 3D tissue constructs using low-viscosity bioink. *Adv. Mater.* **2016**, *28*, 677–684. [CrossRef] [PubMed]

[38] Beyer, S.T.; Mohamed, T.; Waluś, K.J. (Eds.) A microfluidics based 3D bioprinter with on-the-fly multi-material switching capability. In Proceedings of the 17th International Conference on Miniaturized Systems for Chemistry and Life Sciences, Freiburg, Germany, 27–31 October 2013. Available online: https://api.semanticscholar.org/CorpusID:4652749.

[39] Dickman, C.T.D.; Russo, V.; Thain, K.; Pan, S.; Beyer, S.T.; Walus, K.; Getsios, S.; Mohamed, T.; Wadsworth, S.J. Functional characterization of 3D contractile smooth muscle tissues generated using a unique microfluidic 3D bioprinting technology. *FASEB J.* **2020**, *34*, 1652–1664. [CrossRef]

[40] Addario, G.; Djudjaj, S.; Farè, S.; Boor, P.; Moroni, L.; Mota, C. Microfluidic bioprinting towards a renal in vitro model. *Bioprinting* **2020**, *20*, e00108. [CrossRef]

[41] Davoodi, E.; Sarikhani, E.; Montazerian, H.; Ahadian, S.; Costantini, M.; Swieszkowski, W.; Willerth, S.M.; Walus, K.; Mofidfar, M.; Toyserkani, E.; et al. Extrusion and microfluidic-based bioprinting to fabricate biomimetic tissues and organs. *Adv. Mater. Technol.* **2020**, *5*, 1901044. [CrossRef] [PubMed]

[42] Pi, Q.; Maharjan, S.; Yan, X.; Liu, X.; Singh, B.; van Genderen, A.M.; Robledo-Padilla, F.; Parra-Saldivar, R.; Hu, N.; Jia, W.; et al. Digitally tunable microfluidic bioprinting of multilayered cannular tissues. *Adv. Mater.* **2018**, *30*, 1706913. [CrossRef]

[43] Wu, Z.; Cai, H.; Ao, Z.; Xu, J.; Heaps, S.; Guo, F. Microfluidic printing of tunable hollow microfibers for vascular tissue engineering. *Adv. Mater. Technol.* **2021**, *6*, 2000683. [CrossRef]

[44] Zhang, Y.S.; Arneri, A.; Bersini, S.; Shin, S.-R.; Zhu, K.; Goli-Malekabadi, Z.; Aleman, J.; Colosi, C.; Busignani, F.; Dell'Erba, V.; et al. Bioprinting 3D microfibrous scaffolds for engineering endothelialized myocardium and heart-on-a-chip. *Biomaterials* **2016**, *110*, 45–59. [CrossRef] [PubMed]

[45] Hong, S.; Kim, J.S.; Jung, B.; Won, C.; Hwang, C. Coaxial bioprinting of cell-laden vascular constructs using a gelatin–tyramine bioink. *Biomater. Sci.* **2019**, *7*, 4578–4587. [CrossRef] [PubMed]

[46] Gao, G.; Park, W.; Kim, B.S.; Ahn, M.; Chae, S.; Cho, W.-W.; Kim, J.; Lee, J.Y.; Jang, J.; Cho, D.-W. Construction of a novel in vitro atherosclerotic model from geometry-tunable artery equivalents engineered via in-bath coaxial cell printing. *Adv. Funct. Mater.* **2021**, *31*, 2008878. [CrossRef]

[47] Maharjan, S.; He, J.J.; Lv, L.; Wang, D.; Zhang, Y.S. *Microfluidic coaxial bioprinting of hollow, standalone, and perfusable vascular conduits*; Springer US: New York, NY, USA, 2022; pp. 61–75.

[48] Wang, D.; Maharjan, S.; Kuang, X.; Wang, Z.; Mille, L.S.; Tao, M.; Yu, P.; Cao, X.; Lian, L.; Lv, L.; et al. Microfluidic bioprinting of tough hydrogel-based vascular conduits for functional blood vessels. *Sci. Adv.* **2022**, *8*, eabq6900. [CrossRef]

[49] Moragues, T.; Arguijo, D.; Beneyton, T.; Modavi, C.; Simutis, K.; Abate, A.R.; Baret, J.-C.; Demello, A.J.; Densmore, D.; Griffiths, A.D. Droplet-based microfluidics. *Nat. Rev. Methods Primers* **2023**, *3*, 32. [CrossRef]

[50] Hong, G.; Kim, J.; Oh, H.; Yun, S.; Kim, C.M.; Jeong, Y.M.; Yun, W.S.; Shim, J.H.; Jang, I.; Kim, C.Y.; et al. Production of multiple cell-laden microtissue spheroids with a biomimetic hepatic-lobule-like structure. *Adv. Mater.* **2021**, *33*, 2102624. [CrossRef] [PubMed]

[51] Mea, H.J.; Delgadillo, L.; Wan, J. On-demand modulation of 3D-printed elastomers using programmable droplet inclusions. *Proc. Natl. Acad. Sci. USA* **2020**, *117*, 14790–14797. [CrossRef]

[52] Li, X.; Zhang, J.M.; Yi, X.; Huang, Z.; Lv, P.; Duan, H. Multimaterial microfluidic 3D printing of textured composites with liquid inclusions. *Adv. Sci.* **2019**, *6*, 1800730. [CrossRef] [PubMed]

[53] Nelson, A.Z.; Kundukad, B.; Wong, W.K.; Khan, S.A.; Doyle, P.S. Embedded droplet printing in yield-stress fluids. *Proc. Natl. Acad. Sci. USA* **2020**, *117*, 5671–5679. [CrossRef] [PubMed]

[54] Kamperman, T.; Trikalitis, V.D.; Karperien, M.; Visser, C.W.; Leijten, J. Ultrahigh-throughput production of monodisperse and multifunctional Janus microparticles using in-air microfluidics. *ACS Appl. Mater. Interfaces* **2018**, *10*, 23433–23438. [CrossRef] [PubMed]

[55] Walther, A.; Müller, A.H.E. Janus particles: Synthesis, self-assembly, physical properties, and applications. *Chem. Rev.* **2013**, *113*, 5194–5261. [CrossRef] [PubMed]

[56] Wu, Y.; Su, H.; Li, M.; Xing, H. Digital light processing-based multi-material bioprinting: Processes, applications, and perspectives. *J. Biomed. Mater. Res. Part A* **2023**, *111*, 527–542. [CrossRef]

[57] Miri, A.K.; Nieto, D.; Iglesias, L.; Goodarzi Hosseinabadi, H.; Maharjan, S.; Ruiz-Esparza, G.U.; Khoshakhlagh, P.; Manbachi, A.; Dokmeci, M.R.; Chen, S.; et al. Microfluidics-enabled multimaterial maskless stereolithographic bioprinting. *Adv. Mater.* **2018**, *30*, 1800242. [CrossRef]

[58] Nieto, D.; Mora, A.J.d.; Kalogeropoulou, M.; Bhusal, A.; Miri, A.K.; Moroni, L. Bottom-up and top-down VAT photopolymerization bioprinting for rapid fabrication of multi-material microtissues. *Int. J. Bioprinting* **2024**, *10*, 1017. [CrossRef]

[59] Wang, M.; Li, W.; Mille, L.S.; Ching, T.; Luo, Z.; Tang, G.; Garciamendez, C.E.; Lesha, A.; Hashimoto, M.; Zhang, Y.S. Digital light processing based bioprinting with composable gradients. *Adv. Mater.* **2022**, *34*, 2107038. [CrossRef]

[60] Kunwar, P.; Poudel, A.; Aryal, U.; Xie, R.; Geffert, Z.J.; Wittmann, H.; Fougnier, D.; Chiang, T.H.; Maye, M.M.; Li, Z.; et al. Multi-material gradient printing using meniscus-enabled projection stereolithography (MAPS). *Adv. Mater. Technol.* **2024**, 2400675. [CrossRef]

[61] Han, D.; Yang, C.; Fang, N.X.; Lee, H. Rapid multi-material 3D printing with projection micro-stereolithography using dynamic fluidic control. *Addit. Manuf.* **2019**, *27*, 606–615. [CrossRef]

[62] Tobia, J.; Yang, C.; Kim, J.; Han, D.; Lee, H. Material-efficient multimaterial projection micro-stereolithography using droplet-based resin supply. *Int. J. Precis. Eng. Manuf.-Green Technol.* **2024**, *11*, 1071–1079. [CrossRef]

[63] Fournié, V.; Venzac, B.; Trevisiol, E.; Foncy, J.; Roul, J.; Assie-Souleille, S.; Escudero, M.; Joseph, P.; Reitz, A.; Malaquin, L. A microfluidics-assisted photopolymerization method for high-resolution multimaterial 3D printing. *Addit. Manuf.* **2023**, *72*, 103629. [CrossRef]

[64] Juncker, D.; Schmid, H.; Delamarche, E. Multipurpose microfluidic probe. *Nat. Mater.* **2005**, *4*, 622–628. [CrossRef] [PubMed]

[65] Bader, C.; Kolb, D.; Weaver, J.C.; Sharma, S.; Hosny, A.; Costa, J.; Oxman, N. Making data matter: Voxel printing for the digital fabrication of data across scales and domains. *Sci. Adv.* **2018**, *4*, eaas8652. [CrossRef] [PubMed]

[66] Smith, W.A.P. *3D data representation, storage and processing*; Springer International Publishing: New York, NY, USA, 2020; pp. 265–316.

[67] Ahsan, A.M.M.; Xie, R.; Bashir, K. Heterogeneous topology design and voxel-based bio-printing. *Rapid Prototyp. J.* **2018**, *24*, 1142–1154. [CrossRef]

[68] Thijssen, Q.; Toombs, J.; Li, C.C.; Taylor, H.; Van Vlierberghe, S. From pixels to voxels: A mechanistic perspective on volumetric 3D-printing. *Prog. Polym. Sci.* **2023**, *147*, 101755. [CrossRef]

[69] Wickramasinghe, U.; Remelli, E.; Knott, G.; Fua, P. *Voxel2Mesh: 3D mesh model generation from volumetric data*; Springer International Publishing: New York, NY, USA, 2020; pp. 299–308. [CrossRef]

[70] Skylar-Scott, M.A.; Mueller, J.; Visser, C.W.; Lewis, J.A. Voxelated soft matter via multimaterial multinozzle 3D printing. *Nature* **2019**, *575*, 330–335. [CrossRef] [PubMed]

[71] Hassan, I.; Selvaganapathy, P.R. A microfluidic printhead with integrated hybrid mixing by sequential injection for multimaterial 3D printing. *Addit. Manuf.* **2022**, *50*, 102559. [CrossRef]

[72] Zhu, J.; He, Y.; Wang, Y.; Cai, L.-H. Voxelated bioprinting of modular double-network bio-ink droplets. *Nat. Commun.* **2024**, *15*, 5902. [CrossRef]

[73] Zhu, J.; He, Y.; Kong, L.; He, Z.; Kang, K.Y.; Grady, S.P.; Nguyen, L.Q.; Chen, D.; Wang, Y.; Oberholzer, J.; et al. Digital assembly of spherical viscoelastic bio-ink particles. *Adv. Funct. Mater.* **2022**, *32*, 2109004. [CrossRef]

[74] Serex, L.; Sharma, K.; Rizov, V.; Bertsch, A.; McKinney, J.D.; Renaud, P. Microfluidic-assisted bioprinting of tissues and organoids at high cell concentrations. *Biofabrication* **2021**, *13*, 025006. [CrossRef] [PubMed]

[75] Yu, F.; Choudhury, D. Microfluidic bioprinting for organ-on-a-chip models. *Drug Discov. Today* **2019**, *24*, 1248–1257. [CrossRef] [PubMed]

[76] Costantini, M.; Testa, S.; Mozetic, P.; Barbetta, A.; Fuoco, C.; Fornetti, E.; Tamiro, F.; Bernardini, S.; Jaroszewicz, J.; Święszkowski, W.; et al. Microfluidic-enhanced 3D bioprinting of aligned myoblast-laden hydrogels leads to functionally organized myofibers in vitro and in vivo. *Biomaterials* **2017**, *131*, 98–110. [CrossRef]

[77] Miri, A.K.; Khalilpour, A.; Cecen, B.; Maharjan, S.; Shin, S.R.; Khademhosseini, A. Multiscale bioprinting of vascularized models. *Biomaterials* **2019**, *198*, 204–216. [CrossRef] [PubMed]

[78] Di Lullo, E.; Kriegstein, A.R. The use of brain organoids to investigate neural development and disease. *Nat. Rev. Neurosci.* **2017**, *18*, 573–584. [CrossRef] [PubMed]

[79] Li, K.; Gu, L.; Cai, H.; Lu, H.-C.; Mackie, K.; Guo, F. Human brain organoids for understanding substance use disorders. *Drug Metab. Pharmacokinet.* **2024**, 101036. [CrossRef]

[80] Zhao, Z.; Chen, X.; Dowbaj, A.M.; Sljukic, A.; Bratlie, K.; Lin, L.; Fong, E.L.S.; Balachander, G.M.;

Chen, Z.; Soragni, A.; et al. Organoids. *Nat. Rev. Methods Primers* **2022**, *2*, 94. [CrossRef] [PubMed]

[81] Tenreiro, M.F.; Branco, M.A.; Cotovio, J.P.; Cabral, J.M.S.; Fernandes, T.G.; Diogo, M.M. Advancing organoid design through co-emergence, assembly, and bioengineering. *Trends Biotechnol.* **2023**, *41*, 923–938. [CrossRef] [PubMed]

[82] Lancaster, M.A.; Corsini, N.S.; Wolfinger, S.; Gustafson, E.H.; Phillips, A.W.; Burkard, T.R.; Otani, T.; Livesey, F.J.; Knoblich, J.A. Guided self-organization and cortical plate formation in human brain organoids. *Nat. Biotechnol.* **2017**, *35*, 659–666. [CrossRef]

[83] Watanabe, M.; Buth, J.E.; Vishlaghi, N.; De La Torre-Ubieta, L.; Taxidis, J.; Khakh, B.S.; Coppola, G.; Pearson, C.A.; Yamauchi, K.; Gong, D.; et al. Self-organized cerebral organoids with human-specific features predict effective drugs to combat Zika virus infection. *Cell Rep.* **2017**, *21*, 517–532. [CrossRef]

[84] Lei, T.; Zhang, X.; Fu, G.; Luo, S.; Zhao, Z.; Deng, S.; Li, C.; Cui, Z.; Cao, J.; Chen, P.; et al. Advances in human cellular mechanistic understanding and drug discovery of brain organoids for neurodegenerative diseases. *Ageing Res. Rev.* **2024**, *102*, 102517. [CrossRef]

[85] Salewskij, K.; Penninger, J.M. Blood vessel organoids for development and disease. *Circ. Res.* **2023**, *132*, 498–510. [CrossRef]

[86] van den Berg, C.W.; Dumas, S.J.; Little, M.H.; Rabelink, T.J. Challenges in maturation and integration of kidney organoids for stem cell-based renal replacement therapy. *Kidney Int.* 2024, *in press*. [CrossRef] [PubMed]

[87] Pérez-González, A.; Bévant, K.; Blanpain, C. Cancer cell plasticity during tumor progression, metastasis and response to therapy. *Nat. Cancer* **2023**, *4*, 1063–1082. [CrossRef] [PubMed]

[88] Astuti, Y.; Raymant, M.; Quaranta, V.; Clarke, K.; Abudula, M.; Smith, O.; Bellomo, G.; Chandran-Gorner, V.; Nourse, C.; Halloran, C.; et al. Efferocytosis reprograms the tumor microenvironment to promote pancreatic cancer liver metastasis. *Nat. Cancer* **2024**, *5*, 774–790. [CrossRef]

[89] Chen, J.; Liu, G.; Wang, X.; Hong, H.; Li, T.; Li, L.; Wang, H.; Xie, J.; Li, B.; Li, T.; et al. Glioblastoma stem cell-specific histamine secretion drives pro-angiogenic tumor microenvironment remodeling. *Cell Stem Cell* **2022**, *29*, 1531–1546.e7. [CrossRef] [PubMed]

[90] Haas, L.; Elewaut, A.; Gerard, C.L.; Umkehrer, C.; Leiendecker, L.; Pedersen, M.; Krecioch, I.; Hoffmann, D.; Novatchkova, M.; Kuttke, M.; et al. Acquired resistance to anti-MAPK targeted therapy confers an immune-evasive tumor microenvironment and cross-resistance to immunotherapy in melanoma. *Nat. Cancer* **2021**, *2*, 693–708. [CrossRef] [PubMed]

[91] Han, B.; Qu, C.; Park, K.; Konieczny, S.F.; Korc, M. Recapitulation of complex transport and action of drugs at the tumor microenvironment using tumor-microenvironment-on-chip. *Cancer Lett.* **2016**, *380*, 319–329. [CrossRef] [PubMed]

[92] Kasprzak, A. The role of tumor microenvironment cells in colorectal cancer (CRC) cachexia. *Int. J. Mol. Sci.* **2021**, *22*, 1565. [CrossRef]

[93] McLaughlin, M.; Patin, E.C.; Pedersen, M.; Wilkins, A.; Dillon, M.T.; Melcher, A.A.; Harrington, K.J. Inflammatory microenvironment remodelling by tumour cells after radiotherapy. *Nat. Rev. Cancer* **2020**, *20*, 203–217. [CrossRef]

[94] Mu, H.-Y.; Lin, C.-M.; Chu, L.-A.; Lin, Y.-H.; Li, J.; Liu, C.-Y.; Huang, H.-C.; Cheng, S.-L.; Lee, T.-Y.; Lee, H.M.; et al. Ex vivo evaluation of combination immunotherapy using tumor-microenvironment-on-chip. *Adv. Healthc. Mater.* **2024**, *13*, 2302268. [CrossRef]

[95] Mukhopadhyay, M. Synthetic tumor microenvironments. *Nat. Methods* **2021**, *18*, 1274. [CrossRef] [PubMed]

[96] Wang, Y.; Narasimamurthy, R.; Qu, M.; Shi, N.; Guo, H.; Xue, Y.; Barker, N. Circadian regulation of cancer stem cells and the tumor microenvironment during metastasis. *Nat. Cancer* **2024**, *5*, 546–556. [CrossRef]

[97] Wu, H.; Gao, W.; Chen, P.; Wei, Y.; Zhao, H.; Wang, F. Research progress of drug resistance mechanism of temozolomide in the treatment of glioblastoma. *Heliyon* **2024**, *10*, e39984. [CrossRef] [PubMed]

[98] Lee, G.; Kim, S.J.; Park, J.K. Bioprinted multi-composition array mimicking tumor microenvironments to evaluate drug efficacy with multivariable analysis. *Adv. Healthc. Mater.* **2024**, *13*, 2303716. [CrossRef]

[99] Lin, M.; Tang, M.; Duan, W.; Xia, S.; Liu, W.; Wang, Q. 3D bioprinting for tumor metastasis research. *ACS Biomater. Sci. Eng.* **2023**, *9*, 3116–3133. [CrossRef]

[100] Huang, Y.L.; Segall, J.E.; Wu, M. Microfluidic modeling of the biophysical microenvironment in tumor cell invasion. *Lab A Chip* **2017**, *17*, 3221–3233. [CrossRef] [PubMed]

[101] Kim, H.; Sa, J.K.; Kim, J.; Cho, H.J.; Oh, H.J.; Choi, D.H.; Kang, S.H.; Jeong, D.E.; Nam, D.H.; Lee, H.; et al. Recapitulated crosstalk between cerebral metastatic lung cancer cells and brain perivascular tumor microenvironment in a microfluidic co-culture chip. *Adv. Sci.* **2022**, *9*, 2201785. [CrossRef] [PubMed]

[102] Kuang, J.; Sun, W.; Zhang, M.; Kang, L.; Yang, S.; Zhang, H.; Wang, Y.; Hu, P. A three-dimensional biomimetic microfluidic chip to study the behavior of hepatic stellate cell under the tumor microenvironment. *Chin. Chem. Lett.* **2023**, *34*, 107573. [CrossRef]

[103] Onoe, H.; Okitsu, T.; Itou, A.; Kato-Negishi, M.; Gojo, R.; Kiriya, D.; Sato, K.; Miura, S.; Iwanaga, S.; Kuribayashi-Shigetomi, K.; et al. Metre-long cell-laden microfibres exhibit tissue morphologies and functions. *Nat. Mater.* **2013**, *12*, 584–590. [CrossRef]

[104] Hassan, S.; Gomez-Reyes, E.; Enciso-Martinez, E.; Shi, K.; Campos, J.G.; Soria, O.Y.P.; Luna-Cerón, E.; Lee, M.C.; Garcia-Reyes, I.; Steakelum, J.; et al. Tunable and compartmentalized multimaterial bioprinting for complex living tissue constructs. *ACS Appl. Mater. Interfaces* **2022**, *14*, 51602–51618. [CrossRef] [PubMed]

[105] Yin, Y.; Vázquez-Rosado, E.J.; Wu, D.; Viswanathan, V.; Farach, A.; Farach-Carson, M.C.; Harrington, D.A. Microfluidic coaxial 3D bioprinting of cell-laden microfibers and microtubes for salivary gland tissue engineering. *Biomater. Adv.* **2023**, *154*, 213588. [CrossRef] [PubMed]

[106] Bhatia, S.N.; Ingber, D.E. Microfluidic organs-on-chips. *Nat. Biotechnol.* **2014**, *32*, 760–772. [CrossRef] [PubMed]

[107] Zhao, Y.; Wang, E.Y.; Lai, F.B.L.; Cheung, K.; Radisic, M. Organs-on-a-chip: A union of tissue engineering and microfabrication. *Trends Biotechnol.* **2023**, *41*, 410–424. [CrossRef]

[108] Mastrangeli, M.; Millet, S.; Van Den Eijnden-Van Raaij, J. Organ-on-chip in development: Towards a roadmap for organs-on-chip. *ALTEX Altern. Anim. Exp.* **2019**, *36*, 650–668. [CrossRef] [PubMed]

[109] Nahon, D.M.; Moerkens, R.; Aydogmus, H.; Lendemeijer, B.; Martínez-Silgado, A.; Stein, J.M.; Dostanić, M.; Frimat, J.-P.; Gontan, C.; De Graaf, M.N.S.; et al. Standardizing designed and emergent quantitative features in microphysiological systems. *Nat. Biomed. Eng.* **2024**, *8*, 941–962. [CrossRef] [PubMed]

[110] Yang, J.; Hirai, Y.; Iida, K.; Ito, S.; Trumm, M.; Terada, S.; Sakai, R.; Tsuchiya, T.; Tabata, O.; Kamei, K.-I. Integrated-gut-liver-on-a-chip platform as an in vitro human model of non-alcoholic fatty liver disease. *Commun. Biol.* **2023**, *6*, 310. [CrossRef] [PubMed]

[111] Deguchi, S.; Kosugi, K.; Hashimoto, R.; Sakamoto, A.; Yamamoto, M.; Krol, R.P.; Gee, P.; Negoro, R.; Noda, T.; Yamamoto, T.; et al. Elucidation of the liver pathophysiology of COVID-19 patients using liver-on-a-chips. *PNAS Nexus* **2023**, *2*, pgad029. [CrossRef] [PubMed]

[112] Ingber, D.E. Human organs-on-chips for disease modelling, drug development and personalized medicine. *Nat. Rev. Genet.* **2022**, *23*, 467–491. [CrossRef] [PubMed]

[113] Van Den Berg, A.; Mummery, C.L.; Passier, R.; Van Der Meer, A.D. Personalised organs-on-chips: Functional testing for precision medicine. *Lab A Chip* **2019**, *19*, 198–205. [CrossRef]

[114] Pun, S.; Prakash, A.; Demaree, D.; Krummel, D.P.; Sciumè, G.; Sengupta, S.; Barrile, R. Rapid biofabrication of an advanced microphysiological system mimicking phenotypical heterogeneity and drug resistance in glioblastoma. *Adv. Healthc. Mater.* **2024**, *13*, 2401876. [CrossRef]

[115] Hakimi, N.; Cheng, R.; Leng, L.; Sotoudehfar, M.; Ba, P.Q.; Bakhtyar, N.; Amini-Nik, S.; Jeschke, M.G.; Günther, A. Handheld skin printer: In situ formation of planar biomaterials and tissues. *Lab A Chip* **2018**, *18*, 1440–1451. [CrossRef] [PubMed]

[116] Mahmoudi, Z.; Sedighi, M.; Jafari, A.; Naghieh, S.; Stefanek, E.; Akbari, M.; Savoji, H. In situ 3D bioprinting: A promising technique in advanced biofabrication strategies. *Bioprinting* **2023**, *31*, e00260. [CrossRef]

[117] Mohammadi, S.; D'Alessandro, S.; Bini, F.; Marinozzi, F.; Cidonio, G. Development of a microfluidic-assisted open-source 3D bioprinting system (MOS3S) for the engineering of hierarchical tissues. *HardwareX* **2024**, *18*, e00527. [CrossRef]

[118] Zaeri, A.; Zgeib, R.; Cao, K.; Zhang, F.; Chang, R.C. Numerical analysis on the effects of microfluidic-based bioprinting parameters on the microfiber geometrical outcomes. *Sci. Rep.* **2022**, *12*, 3364. [CrossRef] [PubMed]

[119] Mirani, B.; Stefanek, E.; Godau, B.; Hossein Dabiri, S.M.; Akbari, M. Microfluidic 3D printing of a photo-cross-linkable bioink using insights from computational modeling. *ACS Biomater. Sci. Eng.* **2021**, *7*, 3269–3280. [CrossRef] [PubMed]

[120] Jiang, H.; Liu, Z.; Tang, F.; Cheng, Y.; Tian, W.; Shi, W.; Zhang, J.M.; Zhang, Y. A modular and cost-effective droplet microfluidic device for controlled emulsion production. *Polymers* **2024**, *16*, 765. [CrossRef]

[121] Wu, J.; Fang, H.; Zhang, J.; Yan, S. Modular microfluidics for life sciences. *J. Nanobiotechnol.* **2023**, *21*, 85. [CrossRef]

[122] Serpe, F.; Casciola, C.M.; Ruocco, G.; Cidonio, G.; Scognamiglio, C. Microfluidic fiber spinning for 3D bioprinting: Harnessing microchannels to build macrotissues. *Int. J. Bioprint.* **2024**, *10*, 1404. [CrossRef]